J. Fluid Mech. (2009), *vol.* 618, *pp.* 41–70.
doi:10.1017/S0022112008004291 Printed in the United Kingdom

Weakly nonlinear thermoacoustics for stacks with slowly varying pore cross-sections

P. H. M. W. IN 'T PANHUIS[1]† S. W. RIENSTRA[1], J. MOLENAAR[2] AND J. J. M. SLOT[1]

[1]Department of Mathematics and Computer Science, Eindhoven University of Technology, PO Box 513, 5600 MB, Eindhoven, The Netherlands

[2]Biometris, Wageningen University, PO Box 100, 6700 AC, Wageningen, The Netherlands

(Received 3 September 2007 and in revised form 14 August 2008)

A general theory of thermoacoustics is derived for arbitrary stack pores. Previous theoretical treatments of porous media are extended by considering arbitrarily shaped pores with the only restriction that the pore cross-sections vary slowly in the longitudinal direction. No boundary-layer approximation is necessary. Furthermore, the model allows temperature variations in the pore wall. By means of a systematic approach based on dimensional analysis and small parameter asymptotics, we derive a set of ordinary differential equations for the mean temperature and the acoustic pressure and velocity, where the equation for the mean temperature follows as a consistency condition of the assumed asymptotic expansion. The problem of determining the transverse variation is reduced to finding a Green's function for a modified Helmholtz equation and solving two additional integral equations. Similarly the derivation of streaming is reduced to finding a single Green's function for the Poisson equation on the desired geometry.

1. Introduction

The most general interpretation of thermoacoustics, as described by Rott (1980), includes all effects in acoustics in which heat conduction and entropy variations of the (gaseous) medium play a role. In this paper, we will focus specifically on the theoretical basis of thermoacoustic refrigerators, heat pumps or prime movers; the devices that exploit thermoacoustic effects to produce useful refrigeration, heating, or work.

1.1. *A brief history*

Thermoacoustics has a long history that dates back more than two centuries. For the most part, heat-driven oscillations were the subject of these investigations. Some of the earliest experiments include the Rijke tube (Rijke 1859), the Sondhauss tube (Sondhauss 1850) and the Taconis oscillations (Taconis 1949). The reverse process, generating temperature differences using acoustic oscillations, is a relatively new phenomenon. In 1964, Gifford & Longsworth (1966) designed a device called the pulse-tube refrigerator, generating significant cooling. Merkli & Thomann (1975) presented an accurate theory for cooling in a simple cylindrical resonator.

The first qualitative explanation for thermoacoustics was given in 1887 by Lord Rayleigh. In his classical work *The Theory of Sound*, Rayleigh (1945) explains the

† Email address for correspondence: panhuis@gmail.com

production of thermoacoustic oscillations as an interplay between heat fluxes and density variations:

> 'If heat be given to the air at the moment of greatest condensation (compression) or taken from it at the moment of greatest rarefaction (expansion), the vibration is encouraged.'

Rayleigh's qualitative understanding turned out to be correct, but a quantitatively accurate theoretical description of these phenomena was not achieved until much later. After attempts by Kirchhoff (1868) and Kramers (1949), the breakthrough came in 1969, when Rott and coworkers started a series of papers (Rott 1969, 1973, 1975; Rott & Zouzoulas 1976), in which a linear theory of thermoacoustics was derived. The first to give a comprehensive picture, was Swift (1988). He used Rott's theory of thermoacoustic phenomena to design practical thermoacoustic devices. His work includes experimental results, discussions on how to build these devices, and a coherent development of the theory based on Rott's work. Since then, Swift and others have contributed much to the development of thermoacoustic devices. Most of these results have been summarized in Garrett (2004), a review of thermoacoustic engines and refrigerators. Swift (2002) provides a complete introduction to thermoacoustics and treats several kinds of thermoacoustic devices.

1.2. *Scope*

The aim of this work is to derive a general theory of thermoacoustics. In our analysis, we will consider porous media consisting of pores of the type discussed by Arnott, Bass & Raspet (1991), i.e. long pores with arbitrarily shaped pore cross-sections. We extend their results by allowing a slow variation in the pore cross-section in the longitudinal direction. Furthermore, we will also allow temperature dependence of the speed of sound, specific heat, viscosity and thermal conductivity and we eliminate the restriction of constant pore-wall temperature. Then we take the next step and explain how streaming, a non-zero steady mass flux, can be determined through arbitrary cross-sections. Finally, we show how Green's functions can be used to determine the transverse variation of the variables.

The analysis presented here differs from conventional approaches in the sense that dimensional analysis and small-parameter asymptotics are used to construct a weakly nonlinear theory of thermoacoustics, in which streaming is systematically included. This has two main advantages.

(i) Non-dimensionalization allows us to analyse limiting situations in which parameters differ in orders of magnitude, so that we can study the system as a function of parameters connected to geometry, heat transport and viscous effects.

(ii) We can give explicit conditions under which the theory is valid. Furthermore, we can clarify under which conditions additional assumptions or approximations are justified. Olson & Swift (1994) also use dimensionless parameters to analyse thermoacoustic devices, but without trying to construct a complete theory of thermoacoustics.

Previous treatments with variable cross-sections have always been restricted to widely spaced pores (boundary-layer approximation); here, no such assumption is made. A more general formulation would allow stack geometries other than collections of arbitrarily shaped pores. Roh, Raspet & Bass (2007), introduce tortuosity and viscous and thermal dynamic shape factors to extend single pore thermoacoustics to bulk porous medium thermoacoustics. Furthermore, there exist various papers on flow through porous media with random or stochastic properties, that could also be

applied to thermoacoustic configurations. Auriault (2002) gives a clear overview of various techniques that can be used:

Statistic modelling (Kröner 1986);
Self-consistent models (Zaoui 1987);
Volume averaging techniques (Quintard & Whitaker 1993);
Method of homogenization for periodic structures (Auriault 1983).

In addition, Auriault (2002) gives a short explanation of how the method of homogenization can be applied to analyse heat and mass transfer in composite materials. A detailed discussion of methods and results from the theory of homogenization and their applications to flow and transport in porous media can be found in Hornung (1997). Another approach is demonstrated by Kamiński (2002) who combines the homogenization approach with a stochastic description of the physical parameters, to analyse viscous incompressible flow with heat transfer.

Streaming refers to a steady mass-flux density or velocity, usually of second order, that is superimposed on the larger first-order oscillations (Nyborg 1965). With the addition of a steady non-zero mean velocity along X, the gas moves through the tube in a repetitive '102 steps forward, 98 steps backward' manner as described by Swift (2002). Streaming is important as a non-zero mass flux can seriously affect the performance of a thermoacoustic device. It can cause convective heat transfer, which can be a loss, but it can also be essential to transfer heat to and from the environment. Backhauss & Swift (2000), in their analysis of a travelling-wave heat engine, show how streaming can cause significant degradation of the efficiency.

The concept of mass streaming has been discussed by many other authors (e.g. Rott 1974; Olson & Swift 1997; Bailliet *et al.* 2001; Waxler 2001), but restricted to simple geometries such as cylindrical pores or parallel plates, although Olson & Swift (1997) do allow slowly varying cross-sections in the tube. Olson & Swift (1997) show that variable cross-sections can occur in practical geometries and can be used to suppress streaming; a suitable asymmetry in the tube can cause counter-streaming that balances the existing streaming in the tube. Bailliet *et al.* (2001) also take into account the temperature dependence of viscosity and thermal conductivity. The same holds for Rott (1974) and Olson & Swift (1997), but restricted to widely spaced pores.

Apart from mass streaming, many other nonlinearities can be important in practice. Backhauss & Swift (2000), Swift (1992) and Poesse & Garrett (2000) have all shown that at high amplitudes, measurements deviate significantly from predictions by linear theory. Streaming, turbulence, transition effects and higher harmonics are mentioned as main causes for these deviations. Turbulence arises at high Reynolds numbers, where the assumption of laminar flow is no longer valid. It disrupts boundary layers and can negatively affect the heat transfer. Turbulence may also arise owing to abrupt changes in the shape or direction of the channels, which can cause significant losses. Swift (2002) gives some suggestions on how to include turbulence in the modelling, but they are by no means complete. Swift (2002) also gives an overview of other nonlinearities and explains how to fit higher harmonics into the asymptotic framework. Higher harmonics oscillate at integer multiples of the fundamental frequency, and can become important at high amplitudes. Although the higher harmonics affect the performance only in fourth-order corrections, they can interact together to form shock waves. Gusev *et al.* (2000) uses asymptotic theory to analyse the forming of shock front formations. Neither turbulence, nor the higher harmonics and resulting shock waves are included in our analysis.

Section 2 gives a detailed description of the model and an overview of the governing equations, boundary conditions and relevant dimensionless numbers. Then, in § 3, we

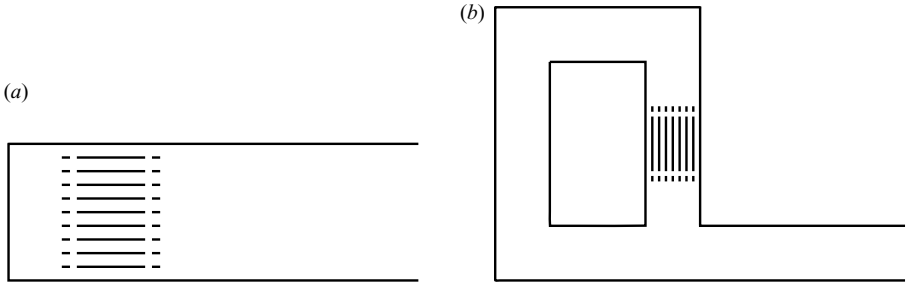

FIGURE 1. Schematic view of two possible duct configurations: (*a*) straight or (*b*) looped.

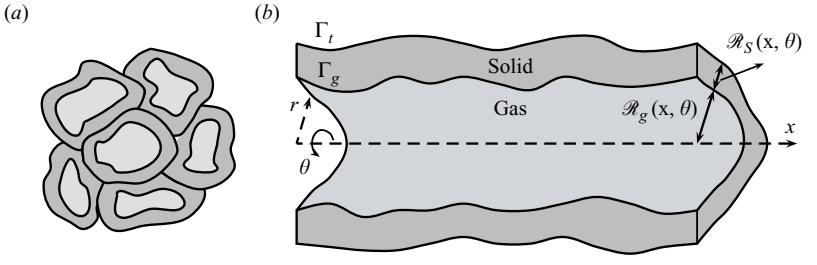

FIGURE 2. Porous medium modelled as a collection of arbitrarily shaped pores. (*a*) Transverse cut of stack; (*b*) Longitudinal cut of one stack pore.

show how these equations simplify inside a narrow tube and we derive equations for the mean and acoustic variables. In § 4 we discuss mass streaming. Then in § 5, we derive an expression for the acoustic power and we show how it is affected by the dimensionless parameters. Finally, in § 6 a short discussion of the results is given.

2. General thermoacoustic theory

2.1. *Geometry*

Thermoacoustic devices are usually of the form shown in figure 1 (Waxler 2001), that is, a (possibly looped) duct containing a fluid (usually a gas) and a porous solid medium, possibly with neighbouring heat exchangers. The duct endings can be both open and closed. For the analysis here we focus on what happens inside the porous medium. We will model the porous medium as a collection of narrow arbitrarily shaped pores aligned in the direction of sound propagation as shown in figure 2. Typical examples are the two-dimensional parallel plates and three-dimensional circular or rectangular pores. Furthermore, we allow the pore boundary to vary slowly (with respect to the channel radius) in the direction of sound propagation, as shown in figure 2(*b*). The system (x, r, θ) forms a cylindrical coordinate system for the stack pore.

In our analysis, we restrict ourselves to one stack pore and its neighbouring solid. Let $\mathscr{A}_g(x)$ denote the gas cross-section and $\mathscr{A}_s(x)$ the half-solid cross-section at position x. Let Γ_g denote the gas–solid interface and Γ_s the outer boundary of the half-solid. We choose Γ_s and $\mathscr{A}_s$ such that at Γ_s the heat flux is zero (for straight pores Γ_s is the centreline of the solid). The remaining stack pores and solid can then be modelled by periodicity. On Γ_g,

$$\mathscr{S}_g(x, r, \theta) := r - \mathscr{R}_g(x, \theta) = 0,$$

with $\mathscr{R}_g(x,\theta)$ the distance of Γ_g to the pore centreline at position x and angle θ. Similarly on Γ_s,

$$\mathscr{S}_t(x,r,\theta) := r - \mathscr{R}_t(x,\theta) = 0,$$

where $\mathscr{R}_t(x,\theta) := \mathscr{R}_g(x,\theta) + \mathscr{R}_s(x,\theta)$ denotes the distance of Γ_s to the origin at position x and angle θ.

Commonly, the porous medium is called a *stack* or a *regenerator* depending on the relative pore width. Following Garrett (2004) we will use the so-called Lautrec number N_L to distinguish between the stack and regenerator. The Lautrec number is defined as the ratio between the pore radius and the thermal penetration depth. If $N_L \sim 1$, the porous medium is called a stack, and if $N_L \ll 1$, it is called a regenerator. If $N_L \gg 1$, as is the case in a resonator, then there is hardly any thermoacoustic effect.

2.2. *Governing equations*

The general equations describing the thermodynamic behaviour in the gas are the well-known conservation laws of mass, momentum and energy (Landau & Lifshitz 1959). Introducing the convective derivative

$$\frac{\mathrm{d}f}{\mathrm{d}t} = \frac{\partial f}{\partial t} + \boldsymbol{v}\cdot\nabla f,$$

these equations can be written in the following form:

$$\text{mass}: \quad \frac{\mathrm{d}\rho}{\mathrm{d}t} = -\rho\nabla\cdot\boldsymbol{v}, \tag{2.1}$$

$$\text{momentum}: \quad \rho\frac{\mathrm{d}\boldsymbol{v}}{\mathrm{d}t} = -\nabla p + \nabla\cdot\boldsymbol{\tau}, \tag{2.2}$$

$$\text{energy}: \quad \rho\frac{\mathrm{d}\epsilon}{\mathrm{d}t} = -\nabla\cdot\boldsymbol{q} - p\nabla\cdot\boldsymbol{v} + \boldsymbol{\tau}:\nabla\boldsymbol{v}. \tag{2.3}$$

Here, ρ is the density, $\boldsymbol{v}$ the velocity, p the pressure, $\boldsymbol{q}$ the heat flux, T the absolute temperature, ϵ the specific internal energy and $\boldsymbol{\tau}$ the viscous stress tensor. For $\boldsymbol{q}$ and $\boldsymbol{\tau}$ we have the following relations:

$$\text{Fourier's heat flux model:} \quad \boldsymbol{q} = -K\nabla T, \tag{2.4}$$

$$\text{Newton's viscous stress tensor:} \quad \boldsymbol{\tau} = 2\mu\boldsymbol{D} + \zeta(\nabla\cdot\boldsymbol{v})\boldsymbol{I}, \tag{2.5}$$

where K is the thermal conductivity, $\boldsymbol{D} = \nabla\boldsymbol{v}/2 + (\nabla\boldsymbol{v})^T/2$ the strain rate tensor, and μ and ζ the dynamic (shear) and second viscosity.

In general, the viscosity and thermal conductivity will depend on temperature. For example, Sutherland's formula (Licht Jr & Stechert 1944) can be used to model the dynamic viscosity as a function of the temperature

$$\mu = \mu^{ref}\frac{1 + S/T^{ref}}{1 + S/T}\left(\frac{T}{T^{ref}}\right)^{1/2},$$

where μ^{ref} is the value of the dynamic viscosity at reference temperature T^{ref} and S is Sutherland's constant. According to Chapman & Cowling (1939), the variation of thermal conductivity is approximately the same as the variation of the viscosity coefficient. The thermodynamic parameters C_p, C_v, β and c may also depend on temperature (see Appendix A). The temperature dependence of μ and K is particularly important, as it allows investigation of Rayleigh streaming: forced convection as a result of viscous and thermal boundary-layer phenomena.

The equations above can be combined and rewritten (Landau & Lifshitz 1959) to yield the following equation for the temperature in the fluid

$$\rho C_p\left(\frac{\partial T}{\partial t}+\boldsymbol{v}\cdot\nabla T\right)=\beta T\left(\frac{\partial p}{\partial t}+\boldsymbol{v}\cdot\nabla p\right)+\nabla\cdot(K\nabla T)+\boldsymbol{\tau}:\nabla\boldsymbol{v}. \tag{2.6}$$

In the solid, we only need an equation for the temperature. The temperature T_s in the solids satisfies the diffusion equation

$$\rho_s C_s\frac{\partial T_s}{\partial t}=\nabla\cdot(K_s\nabla T_s)\,. \tag{2.7}$$

Another useful equation, that can be derived by combining equations (2.1)–(2.3) with the thermodynamic relations from Appendix A, describes the conservation of energy in the following way (Landau & Lifshitz 1959):

$$\frac{\partial}{\partial t}\left(\tfrac{1}{2}\rho|\boldsymbol{v}|^2+\rho\epsilon\right)=-\nabla\cdot\left[\boldsymbol{v}\left(\tfrac{1}{2}\rho|\boldsymbol{v}|^2+\rho h\right)-K\nabla T-\boldsymbol{v}\cdot\boldsymbol{\tau}\right], \tag{2.8}$$

where h is the specific enthalpy.

The equations (2.1), (2.2), (2.6) and (2.7) can be used to determine $\boldsymbol{v}$, p, T and T_s. We should add an equation of state that relates the density to the pressure and temperature in the gas. For the analysis here, it is enough to express the thermodynamic variables ρ, s, ϵ and h in terms of p and T using the thermodynamic equations (A7)–(A10) given in Appendix A. For the numerical examples given in §§ 3.4 and 5.1, it is necessary to make a choice and we choose to impose the ideal gas law,

$$p=\rho(C_p-C_v)T.$$

However, the analysis presented here is also valid for non-ideal gases and nowhere will we use this relation.

To distinguish between variations along and perpendicular to sound propagation we will use a τ in the index to denote the transverse vector components. For example, the transverse gradient and Laplace operators are introduced as follows:

$$\nabla_\tau=\nabla-\frac{\partial}{\partial x}\boldsymbol{e}_x,\qquad \nabla_\tau^2=\nabla^2-\frac{\partial^2}{\partial x^2}.$$

The equations will be linearized and simplified using the following assumptions:

(i) the temperature variations along the stack are much smaller than the average absolute temperature;

(ii) time-dependent variables oscillate with fundamental frequency ω. At the gas–solid interface, we impose the no-slip condition

$$\boldsymbol{v}=\boldsymbol{0},\qquad \text{if}\quad \mathscr{S}_g=0. \tag{2.9}$$

The temperatures in the solid and in the gas are coupled at the gas–solid interface Γ_g where continuity of temperature and heat fluxes is required:

$$T=T_s,\qquad \text{if}\quad \mathscr{S}_g=0, \tag{2.10a}$$

$$K\nabla T\cdot\boldsymbol{n}=K_s\nabla T_s\cdot\boldsymbol{n},\qquad \text{if}\quad \mathscr{S}_g=0. \tag{2.10b}$$

where $\boldsymbol{n}$ is a vector outward normal to the surface. The boundary Γ_s, with outward surface normal $\boldsymbol{n}'$, is chosen such that no heat flux goes through, i.e.

$$\nabla T_s\cdot\boldsymbol{n}'=0,\qquad \text{if}\quad \mathscr{S}_t=0. \tag{2.11}$$

Note that since $\nabla\mathscr{S}_g$ and $\nabla\mathscr{S}_t$ are vectors normal to the surfaces we can also replace the two flux conditions by

$$K\nabla T\cdot\nabla\mathscr{S}_g = K_s\nabla T_s\cdot\nabla\mathscr{S}_g, \quad \text{if} \quad \mathscr{S}_g = 0, \tag{2.12}$$

$$\nabla T_s\cdot\nabla\mathscr{S}_t = 0, \quad \text{if} \quad \mathscr{S}_t = 0. \tag{2.13}$$

2.3. *Non-dimensionalization*

To make the above equations dimensionless, we apply a straightforward scaling procedure. First, we scale time by the frequency of oscillations and the spatial coordinate by a typical pore radius R_g:

$$\mathbf{x} = R_g\tilde{\mathbf{x}}, \qquad t = \frac{1}{\omega}\tilde{t}. \tag{2.14}$$

Note that because we consider narrow stack pores, the typical length scale of radius variation is much larger than a radius. We therefore introduce the small parameter ε as the ratio between a typical radius and this length scale. At Γ_g, we have

$$\tilde{\mathscr{S}}_g(\tilde{X},\tilde{r},\theta) = \tilde{r} - \tilde{\mathscr{R}}_g(X,\theta) = 0, \qquad \tilde{\mathscr{R}}_g(X,\theta) = R_g\mathscr{R}_g(x,\theta), \qquad X = \varepsilon\tilde{x} = Lx.$$

Similarly at Γ_s, we have

$$\tilde{\mathscr{S}}_t(\tilde{X},\tilde{r},\theta) = \tilde{r} - \frac{1}{B_r}\tilde{\mathscr{R}}_t(X,\theta) = 0, \qquad \tilde{\mathscr{R}}_t(X,\theta) = R_t\mathscr{R}_t(x,\theta),$$

where $B_r = R_g/R_t$ is the blockage ratio. Our formal assumption of slow variation has now been made explicit in the slow variable X.

Secondly, we rescale the remaining variables as well, using characteristic values:

$$u = c^{ref}\tilde{u}, \quad \boldsymbol{v}_\tau = \varepsilon c^{ref}\tilde{\boldsymbol{v}}_\tau, \quad p = \rho_g^{ref}(c^{ref})^2\tilde{p}, \quad \boldsymbol{\tau} = \frac{\mu^{ref}c^{ref}}{R_g}\tilde{\boldsymbol{\tau}}, \tag{2.15a}$$

$$\rho = \rho_g^{ref}\tilde{\rho}, \quad T = \frac{(c^{ref})^2}{C_p^{ref}}\tilde{T}, \quad \rho_s = \rho_s^{ref}\tilde{\rho}_s, \quad T_s = \frac{(c^{ref})^2}{C_p^{ref}}\tilde{T}_s, \tag{2.15b}$$

$$h = (c^{ref})^2\tilde{h}, \quad \epsilon = (c^{ref})^2\tilde{\epsilon}, \quad s = C_p^{ref}\tilde{s} \tag{2.15c}$$

$$\beta = \frac{C_p^{ref}}{(c^{ref})^2}\tilde{\beta}, \quad C_p = C_p^{ref}\tilde{C}_p, \quad C_s = C_s^{ref}\tilde{C}_s, \quad c = c^{ref}\tilde{c}, \tag{2.15d}$$

$$K = K^{ref}\tilde{K}, \quad \mu = \mu^{ref}\tilde{\mu}, \quad \zeta = \zeta^{\mathrm{ref}}\tilde{\zeta}. \tag{2.15e}$$

Thirdly, we observe that the system contains 18 parameters, in which 6 physical dimensions are involved. The Buckingham π theorem (Buckingham 1914) implies that the 18 parameters can be combined into 12 independent dimensionless numbers. In table 1, a possible choice is presented. Here, the parameters δ_ν, δ_ζ, δ_k and δ_s are the viscous penetration depths based on dynamic and second viscosity and the thermal penetration depths for the fluid and solid, respectively.

$$\delta_\nu = \sqrt{\frac{2\mu^{ref}}{\omega\rho_g^{ref}}}, \qquad \delta_\zeta = \sqrt{\frac{2\zeta^{\mathrm{ref}}}{\omega\rho_g^{ref}}}, \qquad \delta_k = \sqrt{\frac{2K_g^{ref}}{\omega\rho_g^{ref}C_p^{ref}}}, \qquad \delta_s = \sqrt{\frac{2K_s^{ref}}{\omega\rho_s^{ref}C_s^{ref}}}.$$

Note that 15 dimensionless numbers are introduced. Since at most 12 can be independent, we have at least three dependent numbers. For example, P_r, $\mathscr{S}_k$ and η

Symbol	Formula	Description
γ	C_p^{ref}/C_v^{ref}	Specific heats ratio
η	$(c^{ref}R_g/UL)^2$	ε^2/M_a^2
ε	R_g/L	Stack pore aspect ratio
ϕ	R_s/R_g	Porosity
σ	K_s^{ref}/K_g^{ref}	Ratio thermal conductivities
κ	$\omega L/c^{ref}$	Helmholtz number
B_r	R_g/R_t	Blockage ratio
D_r	p^{osc}/p^{amb}	Drive ratio
M_a	U/c	Mach number
N_L	R_g/δ_k	Lautrec number fluid
N_s	R_s/δ_s	Lautrec number solid
P_r	δ_v^2/δ_k^2	Prandtl number
S_k	$\omega\delta_k/U$	Strouhal number based on δ_k
W_o	$\sqrt{2}R_g/\delta_v$	Womersley number based on μ
W_ζ	$\sqrt{2}R_g/\delta_\zeta$	Womersley number based on ζ

TABLE 1. Dimensionless parameters.

	N_L	M_a	ε	κ	$\mathscr{S}_k$
$\ll 1$	Regenerator	Small velocities	Long pores	Short stack	Thermoacoustic heat flow dominates
~ 1	Stack	Large velocities	Short pores	Long stack	–
$\gg 1$	Resonator	–	–	–	Heat conduction dominates

TABLE 2. Parameter ranges for the important dimensionless parameters.

can be expressed in the other parameters as follows

$$P_r = \frac{2N_L^2}{W_o^2}, \qquad \eta = \frac{\varepsilon^2}{M_a^2}, \qquad \mathscr{S}_k = \frac{\kappa\varepsilon}{N_L M_a}. \tag{2.16}$$

The remaining 12 dimensionless numbers are independent and can be chosen arbitrarily.

In the analysis below, we will use explicitly $M_a \ll 1$ (small velocity amplitudes) and $\varepsilon \ll 1$ (long pores). Other important parameters in thermoacoustics are κ, $\mathscr{S}_k$ and N_L. κ is a Helmholtz number and is therefore a measure for the relative length of the stack with respect to the wavelength; short stacks imply small Helmholtz numbers. In §3.2, it will be shown that $\mathscr{S}_k$ is a measure for the contribution of the thermoacoustic heat flux to the total heat flux in the stack and can be both small and large, depending on the application. As mentioned previously, the Lautrec number distinguishes between the porous medium being a stack ($N_L \sim 1$) or a regenerator ($N_L \ll 1$). These limiting cases are described in table 2.

Hereinafter, we will use dimensionless variables, but omit the tildes for convenience. For ease of notation we also introduce the notation

$$\nabla_\varepsilon = \varepsilon\frac{\partial}{\partial X}\boldsymbol{e}_x + \nabla_\tau, \qquad \boldsymbol{v}_\varepsilon = u\boldsymbol{e}_x + \varepsilon\boldsymbol{v}_\tau.$$

Substituting (2.15) into (2.1)–(2.3), we arrive at the following set of dimensionless equations:

$$\kappa \frac{\partial \rho}{\partial t} + \boldsymbol{v} \cdot \nabla \rho = -\rho \nabla \cdot \boldsymbol{v}, \tag{2.17}$$

$$\rho \left(\kappa \frac{\partial u}{\partial t} + \boldsymbol{v} \cdot \nabla u \right) = -\frac{\partial p}{\partial X} + \frac{\kappa}{W_o^2} \nabla_\varepsilon \cdot (\mu \nabla_\varepsilon u) + \varepsilon^2 \kappa \frac{\partial}{\partial X} \left[\left(\frac{\mu}{W_o^2} + \frac{\zeta}{W_\zeta^2} \right) \nabla \cdot \boldsymbol{v} \right], \tag{2.18}$$

$$\rho \left(\kappa \frac{\partial \boldsymbol{v}_\tau}{\partial t} + \boldsymbol{v} \cdot \nabla \boldsymbol{v}_\tau \right) = -\frac{1}{\varepsilon^2} \nabla_\tau p + \frac{\kappa}{W_o^2} \nabla_\varepsilon \cdot (\mu \nabla_\varepsilon \boldsymbol{v}_\tau) + \kappa \nabla_\tau \left[\left(\frac{\mu}{W_o^2} + \frac{\zeta}{W_\zeta^2} \right) \nabla \cdot \boldsymbol{v} \right], \tag{2.19}$$

$$\rho T \left(\kappa \frac{\partial s}{\partial t} + \boldsymbol{v} \cdot \nabla s \right) = -\frac{\kappa}{2N_L^2} \nabla_\varepsilon \cdot (K \nabla_\varepsilon T) + \kappa \Sigma, \tag{2.20}$$

where

$$\Sigma = \frac{\mu}{W_o^2} \left[\left(\frac{\partial u}{\partial y} + \varepsilon^2 \frac{\partial v}{\partial X} \right)^2 + \left(\frac{\partial u}{\partial z} + \varepsilon^2 \frac{\partial w}{\partial X} \right)^2 + \varepsilon^2 \left(\frac{\partial w}{\partial y} + \frac{\partial v}{\partial z} \right)^2 + 2\varepsilon^2 \left(\left[\frac{\partial u}{\partial X} \right]^2 + \left[\frac{\partial v}{\partial y} \right]^2 + \left[\frac{\partial w}{\partial z} \right]^2 \right) \right] + \frac{\varepsilon^2 \zeta}{W_\zeta^2} (\nabla \cdot \boldsymbol{v})^2 .$$

Equations (2.6) and (2.7) for the fluid and solid temperature transform into

$$\rho C_p \left(\kappa \frac{\partial T}{\partial t} + \boldsymbol{v} \cdot \nabla T \right) = \beta T \left(\kappa \frac{\partial p}{\partial t} + \boldsymbol{v} \cdot \nabla p \right) + \frac{\kappa}{2N_L^2} \nabla_\varepsilon \cdot (K \nabla_\varepsilon T) + \kappa \Sigma, \tag{2.21}$$

$$\rho_s C_s \frac{\partial T_s}{\partial t} = \frac{\phi^2}{2N_s^2} \nabla_\varepsilon \cdot (K_s \nabla_\varepsilon T_s) . \tag{2.22}$$

Furthermore, the conservation of energy (2.8) transforms into

$$\kappa \frac{\partial}{\partial t} \left(\tfrac{1}{2} \rho |\boldsymbol{v}_\varepsilon|^2 + \rho \epsilon \right) = -\nabla_\varepsilon \cdot \left[\frac{\boldsymbol{v}_\varepsilon}{\varepsilon} \left(\tfrac{1}{2} \rho |\boldsymbol{v}_\varepsilon|^2 + \rho h \right) - \frac{\kappa}{2N_L^2} \nabla_\varepsilon T - \frac{\kappa}{W_o^2} \boldsymbol{v}_\varepsilon \cdot \boldsymbol{\tau} \right]. \tag{2.23}$$

Finally, we have the following boundary conditions at the gas–solid interface. First, for the velocity, we have

$$\boldsymbol{v} = 0 \qquad \text{if} \quad \mathscr{S}_g = 0. \tag{2.24a}$$

Second, for the temperature we can write

$$T = T_s \qquad \text{if} \quad \mathscr{S}_g = 0, \tag{2.24b}$$

$$K \nabla_\varepsilon T \cdot \nabla_\varepsilon \mathscr{S}_g = \sigma K_s \nabla_\varepsilon T_s \cdot \nabla_\varepsilon \mathscr{S}_g \qquad \text{if} \quad \mathscr{S}_g = 0. \tag{2.24c}$$

$$\nabla_\varepsilon T_s \cdot \nabla_\varepsilon \mathscr{S}_t = 0, \qquad \text{if} \quad \mathscr{S}_t = 0. \tag{2.24d}$$

2.4. *Small-amplitude and long-pore approximation*

We assume a small amplitude A of acoustic oscillations, i.e. the velocity pressure, density and temperature fluctuations are small relative to their mean value, which can be used to linearize the equations given above. Since all variables are dimensionless, we can use the same A to linearize all variables, e.g. the relative pressure or velocity

amplitude. Let f be any of the fluid variables (p, $\boldsymbol{v}$, T, etc.) with stationary equilibrium profile f_0. Expanding f in powers of A, we have

$$f(\boldsymbol{x},t) = f_0(\boldsymbol{x}) + A\mathrm{Re}\left[f_1(\boldsymbol{x})\mathrm{e}^{\mathrm{i}t}\right] + A^2 f_{2,0}(\boldsymbol{x}) + A^2\mathrm{Re}\left[f_{2,2}(\boldsymbol{x})\mathrm{e}^{2\mathrm{i}t}\right] + \ldots, \qquad A \ll 1,$$

Furthermore, for the velocity we assume $\boldsymbol{v}_0 = 0$. As the velocity was scaled with the speed of sound, the obvious choice for A then becomes the acoustic Mach number M_a, and we will therefore use the following expansion:

$$f(\boldsymbol{x},t) = f_0(\boldsymbol{x}) + M_a\mathrm{Re}\left[f_1(\boldsymbol{x})\mathrm{e}^{\mathrm{i}t}\right] + M_a^2 f_{2,0}(\boldsymbol{x}) + M_a^2\mathrm{Re}\left[f_{2,2}(\boldsymbol{x})\mathrm{e}^{2\mathrm{i}t}\right] + \ldots, \qquad M_a \ll 1, \quad (2.25)$$

The first index is used to indicate the corresponding power of M_a, and the index after the comma is used to indicate the frequency of the oscillation (Swift (2002)). Here, we assumed a harmonic time-dependence for the first-order fluid variables with dimensionless frequency 1 (i.e. dimensional frequency ω). Furthermore, for the second-order fluid variables, we have the combined effect of the second harmonic $f_{2,2}$, which oscillates at twice the fundamental frequency, and the steady streaming part $f_{2,0}$. We assume that the first harmonic $f_{2,1}$ is not excited. In our analysis, we will express the streaming variables in terms of the f_0 and f_1 variables. The second harmonic $f_{2,2}$ is in fact of no interest for the analysis here, but nevertheless it is included for the sake of completeness.

Note that for the analysis in the next sections, we need to know only the leading-order approximation of the thermodynamic parameters c, β, C_p and C_v. The index 0 will therefore be omitted.

Additionally, since we also assume $\varepsilon \ll 1$, we may expand the perturbation variables f_i again to include powers of ε as well. However, this would lead to messy derivations. Instead, we will assume that $\varepsilon \sim M_a$, so that the geometric and streaming effect can be included at the same order. In the end, after all the analysis has been performed, we can still put $\varepsilon \ll M_a$ or $\varepsilon \gg M_a$.

We will use an overbar to indicate time-averaging, and brackets to indicate transverse averaging in the gas, i.e.

$$\overline{f}(\boldsymbol{x}) = \frac{1}{2\pi}\int_0^{2\pi} f(\boldsymbol{x},t)\,\mathrm{d}t, \qquad \langle f\rangle(X,t) = \frac{1}{A_g(X)}\int_{\mathscr{A}_g(X)} f(\boldsymbol{x},t)\,\mathrm{d}A,$$

where A_g is the area of $\mathscr{A}_g$. The time-average of a harmonic variable always yields zero, since $\overline{\mathrm{Re}[a\mathrm{e}^{\mathrm{j}it}]} \equiv 0$, for any $j \in \mathbb{N}$, $a \in \mathbb{C}$. However, the time-average of the product of two harmonic variables is, in general, not equal to zero, as

$$\overline{\mathrm{Re}[f_1\mathrm{e}^{\mathrm{i}t}]\mathrm{Re}[g_1\mathrm{e}^{\mathrm{i}t}]} = \tfrac{1}{2}\mathrm{Re}[f_1 g_1^*] = \tfrac{1}{2}\mathrm{Re}[f_1^* g_1]. \quad (2.26)$$

Here the * denotes complex conjugation.

3. Thermoacoustics in a pore

In this section, a coupled system of ordinary differential equations will be derived for T_0, p_1, $\langle u_1\rangle$ and an auxiliary variable $\mathscr{V}$ to include the effect of cross-sectional variations. Furthermore, several F_j-functions will be introduced that contain the transverse variations of the acoustic variables.

3.1. *Acoustics*

We follow an approach similar to that of Arnott *et al.* (1991). First, we introduce some auxiliary functions. Define α_ν, α_k and α_s as follows:

$$\alpha_\nu = (1+\mathrm{i})\sqrt{\frac{\rho_0}{2\mu_0}}W_o, \qquad \alpha_k = (1+\mathrm{i})\sqrt{\frac{\rho_0}{K_0 C_p}}N_L, \qquad \alpha_s = (1+\mathrm{i})\phi\sqrt{\frac{\rho_{s_0}}{K_{s_0}C_s}}N_s.$$

Given the differential operators $\mathscr{L}_j := \boldsymbol{I} - 1/\alpha_j^2\nabla_\tau^2$ $(j=\nu,k)$ we take F_j $(j=\nu,k)$ such that

$$\mathscr{L}_j[F_j] = 1, \qquad \text{in} \quad \mathscr{A}_g, \tag{3.1a}$$

$$F_j = 0, \qquad \text{on} \quad \Gamma_g. \tag{3.1b}$$

Note that Arnott *et al.* (1991) adopt a slightly different notation; $F(\boldsymbol{x};\alpha_j)$ instead of F_j. Also there is an additional minus-sign in (3.1*a*) because they assume a time-dependence of the form $\mathrm{e}^{-\mathrm{i}t}$, whereas we follow the conventional notation $\mathrm{e}^{\mathrm{i}t}$ of Rott (1969) and Swift (1988).

Now expand the fluid variables in powers of M_a as shown in (2.25). Substituting the expansions into the transverse components of the momentum equation (2.19), putting $\varepsilon^2 = \eta M_a^2$, and keeping terms up to first order in M_a we find

$$0 = -\nabla_\tau p_0 - M_a \nabla_\tau p_1.$$

Collecting the leading-order terms in M_a we find we find that $\nabla_\tau p_0 = 0$, so that p_0 is a function of X only. Furthermore, collecting the first-order terms in M_a, we additionally find that $\nabla_\tau p_1 = 0$, so that p_1 is also a function of X only.

Collecting first-order terms in M_a, we find that the X-component of the momentum equation (2.18) transforms into

$$\mathrm{i}M_a\kappa\rho_0 u_1 = -\frac{\mathrm{d}p_0}{\mathrm{d}X} - M_a\frac{\mathrm{d}p_1}{\mathrm{d}X} + M_a\frac{\kappa}{W_o^2}\nabla_\tau\cdot(\mu_0\nabla_\tau u_1).$$

To leading order, we find that $\mathrm{d}p_0/\mathrm{d}X = 0$ and therefore p_0 is constant. Next, assume that the mean temperature T_0 is a function of X only. Below, we will show that this is indeed the case. As a result, we also find that $\mu_0 = \mu_0(X)$ and $K = K_0(X)$. Then, collecting the terms of first order in M_a, we find that u_1 satisfies

$$u_1 = \frac{\mathrm{i}}{\kappa\rho_0}\frac{\mathrm{d}p_1}{\mathrm{d}X} + \frac{1}{\alpha_\nu^2}\nabla_\tau^2 u_1. \tag{3.2}$$

With the help of (3.1), we can integrate (3.2) subject to $\boldsymbol{v}|_{\Gamma_g} = 0$ and write u_1 and $\mathrm{d}p_1/\mathrm{d}x$ as

$$u_1 = \frac{\mathrm{i}F_\nu}{\kappa\rho_0}\frac{\mathrm{d}p_1}{\mathrm{d}X}, \qquad \langle u_1\rangle = \frac{\mathrm{i}(1-f_\nu)}{\kappa\rho_0}\frac{\mathrm{d}p_1}{\mathrm{d}X}. \tag{3.3}$$

Next, we turn to the temperature equation. Substituting our expansions into (2.21) and (2.22), and keeping terms up to first order in M_a, we find

$$M_a\rho_0 C_p(\mathrm{i}\kappa T_1 + \boldsymbol{v}_1\cdot\nabla T_0) = \mathrm{i}M_a\kappa\beta T_0 p_1 + \frac{\kappa}{2N_L^2}\nabla_\tau\cdot[K_0\nabla_\tau(T_0 + M_a T_1)],$$

$$\mathrm{i}M_a\rho_{s_0}C_s T_{s_1} = \frac{\phi^2}{2N_s^2}\nabla_\tau\cdot[K_{s_0}\nabla_\tau(T_{s_0} + M_a T_{s_1})].$$

To leading order, this reduces to $\nabla_\tau^2 T_0 = \nabla_\tau^2 T_{s_0} = 0$. An obvious solution, satisfying the boundary conditions given in (2.24), is that T_{s_0} and T_0 are equal and independent

of $\boldsymbol{x}_\tau$. In view of the thermodynamic relation (A 8), it also holds that ρ_0 and ρ_{s_0} are independent of $\boldsymbol{x}_\tau$.

Next, collecting the terms of first order in M_a, we find that T_1 and T_{s_1} can be obtained from

$$T_1 + \frac{1}{\kappa^2\rho_0}\frac{\mathrm{d}T_0}{\mathrm{d}X}\frac{\mathrm{d}p_1}{\mathrm{d}X}F_v - \frac{\beta T_0}{\rho_0 C_p}p_1 = \frac{1}{\alpha_k^2}\nabla_\tau^2 T_1, \tag{3.4a}$$

$$T_{s_1} = \frac{1}{\alpha_s^2}\nabla_\tau^2 T_{s_1}, \tag{3.4b}$$

where we substituted (3.3) for u_1.

To solve the temperature from (3.4), we must first introduce some additional auxiliary functions. Arnott *et al.* (1991) solve the differential equations (3.4) using the boundary condition $T|_{\Gamma_g} = 0$, which allows a solution as a combination of F_v and F_k-functions. However, with the boundary conditions given in (2.24), this approach will not work here. Assume for now the boundary function $g := T_1|_{\Gamma_g}$ is known and choose g_p and g_u such that

$$g = g_p\frac{\beta T_0}{\rho_0 c^2}p_1 - \frac{g_u}{\kappa^2(1-P_r)\rho_0}\frac{\mathrm{d}T_0}{\mathrm{d}X}\frac{\mathrm{d}p_1}{\mathrm{d}X}.$$

We can now write for the temperature

$$T_1(\boldsymbol{x}) = \frac{\beta T_0 F_{kp}}{\rho_0 C_p}p_1 - \frac{F_{ku} - P_r F_v}{\kappa^2(1-P_r)\rho_0}\frac{\mathrm{d}T_0}{\mathrm{d}X}\frac{\mathrm{d}p_1}{\mathrm{d}X}, \tag{3.5}$$

$$T_{s_1}(\boldsymbol{x}) = \frac{\beta T_0}{\rho_0 C_p}(1-F_{sp})p_1 - \frac{1-F_{su}}{\kappa^2(1-P_r)\rho_0}\frac{\mathrm{d}T_0}{\mathrm{d}X}\frac{\mathrm{d}p_1}{\mathrm{d}X}, \tag{3.6}$$

where F_{kj} $(j = p, u)$ satisfies

$$\mathscr{L}_k[F_{kj}] = -1 \qquad \text{in} \quad \mathscr{A}_g, \tag{3.7a}$$

$$F_{kj} = g_j \qquad \text{on} \quad \Gamma_g, \tag{3.7b}$$

and F_{sj} $(j = p, u)$ is found from

$$\mathscr{L}_s[F_{sj}] = -1 \qquad \text{in} \quad \mathscr{A}_s, \tag{3.8a}$$

$$F_{sj} = 1 - g_j \qquad \text{on} \quad \Gamma_g, \tag{3.8b}$$

$$\nabla_\tau F_{sj}\cdot\boldsymbol{n}'_\tau = 0 \qquad \text{on} \quad \Gamma_t. \tag{3.8c}$$

The standard way of solving such boundary-value problems is to make use of the Green's functions for the given Helmholtz equations on a cross-section with appropriate boundary conditions. In Appendix B we will show how the g_j and F_{ij} functions can be determined using Green's functions.

Using relations (A 5) and (A 8) and substituting T_1, we can derive the following relation for the acoustic density fluctuations:

$$\rho_1 = \frac{1}{c^2}[\gamma - (\gamma-1)F_{kp}]p_1 + \frac{\beta(F_{ku} - P_r F_v)}{\kappa^2(1-P_r)}\frac{\mathrm{d}T_0}{\mathrm{d}X}\frac{\mathrm{d}p_1}{\mathrm{d}X}. \tag{3.9}$$

Finally, we turn to the continuity equation (2.17). Expanding the variables in powers of M_a and keeping terms up to first order in M_a, we find

$$\mathrm{i}M_a\kappa\rho_1 + M_a\frac{\partial}{\partial X}(\rho_0 u_1) + M_a\rho_0\nabla_\tau\cdot\boldsymbol{v}_{\tau_1} = 0. \tag{3.10}$$

Next, we substitute (3.3). First, note that because of the divergence theorem,

$$\int_{\mathscr{A}_g} \nabla_\tau \cdot \boldsymbol{v}_\tau = \int_{\Gamma_g} \boldsymbol{v}_\tau \cdot \boldsymbol{n} = 0,$$

since $\boldsymbol{v}|_{\Gamma_g} = 0$. Therefore, averaging (3.10) over a cross-section and multiplying with $-\mathrm{i}\kappa$, we obtain the following equation as a consistency relation for v_1:

$$\kappa^2 \langle \rho_1 \rangle + \frac{1}{A_g} \frac{\mathrm{d}}{\mathrm{d}X} \left(A_g (1 - f_v) \frac{\mathrm{d}p_1}{\mathrm{d}X} \right) = 0.$$

After substituting (3.9) and putting $f_j = 1 - \langle F_j \rangle$ ($j = v, kp, ku$), we obtain

$$\frac{\kappa^2}{c^2}[1 + (\gamma - 1) f_{kp}] p_1 + \frac{\beta (f_v - f_{ku})}{1 - P_r} \frac{\mathrm{d}T_0}{\mathrm{d}X} \frac{\mathrm{d}p_1}{\mathrm{d}X} + \beta (1 - f_v) \frac{\mathrm{d}T_0}{\mathrm{d}X} \frac{\mathrm{d}p_1}{\mathrm{d}X} + \frac{1}{A_g} \frac{\mathrm{d}}{\mathrm{d}X} \left(A_g (1 - f_v) \frac{\mathrm{d}p_1}{\mathrm{d}X} \right) = 0.$$

Eventually using

$$\rho_0 \frac{\mathrm{d}}{\mathrm{d}X} \left(\frac{1}{\rho_0} \right) = -\frac{1}{\rho_0} \frac{\mathrm{d}\rho_0}{\mathrm{d}X} = -\frac{1}{\rho_0} \frac{\partial \rho_0}{\partial T_0} \frac{\mathrm{d}T_0}{\mathrm{d}X} = \beta \frac{\mathrm{d}T_0}{\mathrm{d}X}, \tag{3.11}$$

we obtain the dimensionless equivalent of Rott's wave equation for general porous media

$$\frac{\kappa^2}{c^2}[1 + (\gamma - 1) f_{kp}] p_1 + \frac{\beta (f_v - f_{ku})}{1 - P_r} \frac{\mathrm{d}T_0}{\mathrm{d}X} \frac{\mathrm{d}p_1}{\mathrm{d}X} + \frac{\rho_0}{A_g} \frac{\mathrm{d}}{\mathrm{d}X} \left(A_g \frac{1 - f_v}{\rho_0} \frac{\mathrm{d}p_1}{\mathrm{d}X} \right) = 0. \tag{3.12}$$

We can now combine (3.3) and (3.12) to find a coupled system of first-order differential equations for p_1 and $\langle u_1 \rangle$. From (3.3), we find

$$\frac{\rho_0}{A_g} \frac{\mathrm{d}}{\mathrm{d}X} \left(A_g \frac{1 - f_v}{\rho_0} \frac{\mathrm{d}p_1}{\mathrm{d}X} \right) = -\mathrm{i}\kappa \frac{\rho_0}{A_g} \frac{\mathrm{d}}{\mathrm{d}X} (A_g \langle u_1 \rangle). \tag{3.13}$$

Substituting this into (3.12), we find that

$$\frac{\mathrm{d}\langle u_1 \rangle}{\mathrm{d}X} = -\frac{\mathrm{i}\kappa}{\rho_0 c^2}[1 + (\gamma - 1) f_{kp}] p_1 - \left(\frac{\beta (f_v - f_{ku})}{(1 - P_r)(1 - f_v)} \frac{\mathrm{d}T_0}{\mathrm{d}X} + \frac{1}{A_g} \frac{\mathrm{d}A_g}{\mathrm{d}X} \right) \langle u_1 \rangle, \tag{3.14}$$

and, repeating (3.3), we also have

$$\frac{\mathrm{d}p_1}{\mathrm{d}X} = -\frac{\mathrm{i}\kappa \rho_0}{1 - f_v} \langle u_1 \rangle. \tag{3.15}$$

To complete the system of equations, it still remains to find an equation for the mean temperature T_0. The next section explains how this can be done.

3.2. *Mean temperature by the method of slow variation*

Here, we will use (2.23) to determine the mean temperature T_0. In calculating $T_{2,0}$, a consistency relation will be derived that determines T_0. The method adopted here is also referred to as *the method of slow variation* (Van Dyke 1987; Mattheij, Rienstra & ten Thije Boonkkamp 2005).

Putting $\varepsilon^2 = \eta M_a^2$, we can rewrite (2.23) as follows:

$$\kappa \frac{\partial}{\partial t}\left(\tfrac{1}{2}\rho\left(|\boldsymbol{u}|^2 + \eta M_a^2|\boldsymbol{v}_\tau|^2\right) + \rho\epsilon\right)$$
$$= -\frac{\partial}{\partial X}\left(\tfrac{1}{2}\rho u\left(|\boldsymbol{u}|^2 + \eta M_a^2|\boldsymbol{v}_\tau|^2\right) + \rho u h - M_a^2 \frac{\kappa\eta K}{2N_L^2}\frac{\partial T}{\partial X}\right)$$
$$-\nabla_\tau \cdot \left(\tfrac{1}{2}\rho \boldsymbol{v}_\tau\left(|\boldsymbol{u}|^2 + \eta M_a^2|\boldsymbol{v}_\tau|^2\right) + \rho \boldsymbol{v}_\tau h - \frac{\kappa K}{2N_L^2}\nabla_\tau T - \frac{\kappa\mu}{W_o^2} u\nabla_\tau u\right) + \nabla\cdot\mathscr{T},$$

with

$$\mathscr{T} = M_a^2\eta\kappa\begin{bmatrix} \dfrac{\mu}{W_o^2}\left(u\dfrac{\partial u}{\partial X} + \eta M_a^2 \boldsymbol{v}_\tau\cdot\dfrac{\partial \boldsymbol{v}_\tau}{\partial X} + \boldsymbol{v}\cdot\nabla u\right) + \dfrac{\zeta}{W_\zeta^2}u\nabla\cdot\boldsymbol{v} \\ \dfrac{\mu}{W_o^2}\left(\boldsymbol{v}_\tau\cdot\nabla_\tau\boldsymbol{v}_\tau + \boldsymbol{v}\cdot\nabla\boldsymbol{v}_\tau\right) + \dfrac{\zeta}{W_\zeta^2}\boldsymbol{v}_\tau\nabla\cdot\boldsymbol{v} \end{bmatrix}.$$

Averaged in time, the left-hand side of this equation will drop out. Consequently, on expanding in powers of M_a and keeping terms up to second order, we can neglect the $\mathscr{T}$-term and find

$$\frac{\partial}{\partial X}\left[M_a^2\rho_0\overline{u_1 h_1} + M_a^2 h_0 \dot{m}_2 - M_a^2\frac{\kappa\eta K_0}{2N_L^2}\frac{\mathrm{d}T_0}{\mathrm{d}X}\right] + \nabla_\tau\cdot\left[M_a^2\rho_0\overline{\boldsymbol{v}_{\tau_1}h_1} + M_a^2 h_0\dot{\boldsymbol{m}}_{\tau_2}\right.$$
$$\left. - M_a^2\frac{\kappa K_0}{2N_L^2}\nabla_\tau T_{2,0} - M_a^2\frac{\kappa}{2N_L^2}\overline{K_1\nabla_\tau T_1} - M_a^2\frac{\kappa\mu_0}{W_o^2}\overline{u_1\nabla_\tau u_1}\right] = 0,$$

where $\dot{m}_2$ and $\dot{\boldsymbol{m}}_{\tau_2}$ are the components in the longitudinal and transverse directions of the second-order time-averaged mass flux $\dot{\boldsymbol{m}}_2$,

$$\dot{\boldsymbol{m}}_2 := \overline{\rho_0(\boldsymbol{v}_{2,0} + \mathrm{Re}[\boldsymbol{v}_{2,2}\mathrm{e}^{2\mathrm{i}t}]) + \mathrm{Re}[\rho_1\mathrm{e}^{\mathrm{i}t}]\mathrm{Re}[\boldsymbol{v}_1\mathrm{e}^{\mathrm{i}t}]} = \rho_0\boldsymbol{v}_{2,0} + \tfrac{1}{2}\mathrm{Re}[\rho_1\boldsymbol{v}_1^*].$$

Plugging in relation (2.26) and rearranging terms, we find

$$K_0\nabla_\tau^2 T_{2,0} + \tfrac{1}{2}\nabla_\tau\cdot\mathrm{Re}\left[K_1^*\nabla_\tau T_1\right] + \eta\frac{\mathrm{d}}{\mathrm{d}X}\left(K_0\frac{\mathrm{d}T_0}{\mathrm{d}X}\right) = \frac{N_L^2}{\kappa}\frac{\partial}{\partial X}(\rho_0\mathrm{Re}[u_1^* h_1] + 2h_0\dot{m}_2)$$
$$+ \frac{N_L^2}{\kappa}\nabla_\tau\cdot(\rho_0\mathrm{Re}[\boldsymbol{v}_{\tau_1}^* h_1] + 2h_0\dot{\boldsymbol{m}}_{\tau_2} - \frac{\kappa}{W_o^2}\mathrm{Re}[u_1^*\nabla_\tau u_1]). \quad (3.16)$$

Similarly, we can show in the solid that (2.22) reduces to

$$K_{s_0}\nabla_\tau^2 T_{s_{2,0}} + \tfrac{1}{2}\nabla_\tau\cdot\mathrm{Re}[K_{s_1}^*\nabla_\tau T_{s_1}] + \eta\frac{\mathrm{d}}{\mathrm{d}X}\left(K_{s_0}\frac{\mathrm{d}T_0}{\mathrm{d}X}\right) = 0. \quad (3.17)$$

We will now use the flux condition (2.24*c*) to derive a differential equation for T_0. Time-averaging and expanding (2.24*c*) in powers of M_a and collecting the second-order terms in M_a, we find

$$(K_0\nabla_\tau T_{2,0} + \tfrac{1}{2}\mathrm{Re}[K_1^*\nabla_\tau T_1] - \sigma K_{s_0}\nabla_\tau T_{s_{2,0}} - \sigma\tfrac{1}{2}\mathrm{Re}[K_{s_1}^*\nabla_\tau T_{s_1}])\cdot\nabla_\tau\mathscr{S}_g$$
$$= gs(\sigma K_{s_0} - K_0)\frac{\mathrm{d}T_0}{\mathrm{d}X}\frac{\partial\mathscr{S}_g}{\partial X}, \qquad \mathscr{S}_g = 0.$$

This condition can be rewritten as

$$(K_0\nabla_\tau T_{2,0} + \tfrac{1}{2}\mathrm{Re}[K_1^*\nabla_\tau T_1] - \sigma K_{s_0}\nabla_\tau T_{s_{2,0}} - \sigma\tfrac{1}{2}\mathrm{Re}[K_{s_1}^*\nabla_\tau T_{s_1}])\cdot\boldsymbol{n}_\tau$$
$$= \eta\frac{K_0-\sigma K_{s_0}}{|\nabla_\tau \mathscr{S}_g|}\frac{\partial \mathscr{R}_g}{\partial X}\frac{\mathrm{d}T_0}{\mathrm{d}X} = \eta\frac{(K_0-\sigma K_{s_0})\mathscr{R}_g}{\sqrt{\mathscr{R}_g^2+(\partial\mathscr{R}_g/\partial\theta)^2}}\frac{\partial \mathscr{R}_g}{\partial X}\frac{\mathrm{d}T_0}{\mathrm{d}X}, \qquad \mathscr{S}_g = 0, \quad (3.18)$$

where $\boldsymbol{n}_\tau := \nabla_\tau\mathscr{S}_g/(\nabla_\tau\mathscr{S}_g)$ is the outward unit normal vector to Γ_g. Similarly, since $\boldsymbol{n}'_\tau := \nabla_\tau\mathscr{S}_t/(\nabla_\tau\mathscr{S}_t)$ is the outward unit normal vector to Γ_s, we find from (2.24*d*)

$$K_{s_0}\nabla T_{s_{2,0}}\cdot\boldsymbol{n}'_\tau + \tfrac{1}{2}\nabla_\tau\cdot\mathrm{Re}[K_{s_1}^*\nabla_\tau T_{s_1}] = \frac{\eta K_{s_0}\mathscr{R}_t}{\sqrt{\mathscr{R}_t^2+(\partial\mathscr{R}_t/\partial\theta)^2}}\frac{\partial\mathscr{R}_t}{\partial X}\frac{\mathrm{d}T_0}{\mathrm{d}X}, \qquad \mathscr{S}_t = 0. \quad (3.19)$$

Now on the one hand, by applying the divergence theorem, substituting the flux conditions (3.18) and (3.19), and noting that $A = (1/2)\int_0^{2\pi}\mathscr{R}^2\,\mathrm{d}\theta$ and $\mathrm{d}\ell = (\mathscr{R}^2 + (\partial\mathscr{R}/\partial\theta)^2)^{1/2}\mathrm{d}\theta$, we find

$$\int_{\mathscr{A}_g}\left(K_0\nabla_\tau^2 T_{2,0} + \tfrac{1}{2}\nabla_\tau\cdot\mathrm{Re}\left[K_1^*\nabla_\tau T_1\right] + \eta\frac{\mathrm{d}}{\mathrm{d}X}\left(K_0\frac{\mathrm{d}T_0}{\mathrm{d}X}\right)\right)\mathrm{d}S$$
$$+\sigma\int_{\mathscr{A}_s}\left(K_{s_0}\nabla_\tau^2 T_{s_{2,0}} + \tfrac{1}{2}\nabla_\tau\cdot\mathrm{Re}\left[K_{s_1}^*\nabla_\tau T_{s_1}\right] + \eta\frac{\mathrm{d}}{\mathrm{d}X}\left(K_{s_0}\frac{\mathrm{d}T_0}{\mathrm{d}X}\right)\right)\mathrm{d}S$$
$$= \int_{\Gamma_g}\left(K_0\nabla_\tau T_{2,0} + \tfrac{1}{2}\mathrm{Re}[K_1^*\nabla_\tau T_1] - \sigma K_{s_0}\nabla_\tau T_{s_{2,0}} - \tfrac{1}{2}\sigma\mathrm{Re}[K_{s_1}^*\nabla_\tau T_{s_1}]\right)\cdot\boldsymbol{n}_\tau\,\mathrm{d}\ell$$
$$+\sigma\int_{\Gamma_s}\left(K_{s_0}\nabla\mathscr{T}_{s_2} + \tfrac{1}{2}\mathrm{Re}[K_{s_1}^*\nabla_\tau T_{s_1}]\right)\cdot\boldsymbol{n}'_\tau\,\mathrm{d}\ell$$
$$+\eta A_g\frac{\mathrm{d}}{\mathrm{d}X}\left(K_0\frac{\mathrm{d}T_0}{\mathrm{d}X}\right) + \eta\sigma A_s\frac{\mathrm{d}}{\mathrm{d}X}\left(K_{s_0}\frac{\mathrm{d}T_0}{\mathrm{d}X}\right)$$
$$= \eta(K_0-\sigma K_{s_0})\frac{\mathrm{d}T_0}{\mathrm{d}X}\int_0^{2\pi}\mathscr{R}_g\frac{\partial\mathscr{R}_g}{\partial X}\mathrm{d}\theta + \eta\sigma K_{s_0}\frac{\mathrm{d}T_0}{\mathrm{d}X}\int_0^{2\pi}\mathscr{R}_t\frac{\partial\mathscr{R}_t}{\partial X}\mathrm{d}\theta$$
$$+\eta A_g\frac{\mathrm{d}}{\mathrm{d}X}\left(K_0\frac{\mathrm{d}T_0}{\mathrm{d}X}\right) + \eta\sigma A_s\frac{\mathrm{d}}{\mathrm{d}X}(K_{s_0}\frac{\mathrm{d}T_0}{\mathrm{d}X})$$
$$= \eta\frac{\mathrm{d}}{\mathrm{d}X}\left[\left(K_0A_g + \sigma K_{s_0}A_s\right)\frac{\mathrm{d}T_0}{\mathrm{d}X}\right]. \quad (3.20)$$

On the other hand, combining (3.16) and (3.17), applying the divergence theorem and using $\boldsymbol{v}|_{\Gamma_g} = 0$, we also have

$$\int_{\mathscr{A}_g}\left(K_0\nabla_\tau^2 T_{2,0} + \tfrac{1}{2}\nabla_\tau\cdot\mathrm{Re}[K_1^*\nabla_\tau T_1] + \eta\frac{\mathrm{d}}{\mathrm{d}X}\left(K_0\frac{\mathrm{d}T_0}{\mathrm{d}X}\right)\right)\mathrm{d}S$$
$$+\sigma\int_{\mathscr{A}_s}\left(K_{s_0}\nabla_\tau^2 T_{s_{2,0}} + \tfrac{1}{2}\nabla_\tau\cdot\mathrm{Re}[K_{s_1}^*\nabla_\tau T_{s_1}] + \eta\frac{\mathrm{d}}{\mathrm{d}X}\left(K_{s_0}\frac{\mathrm{d}T_0}{\mathrm{d}X}\right)\right)\mathrm{d}S$$
$$= \frac{N_L^2}{\kappa}\int_{\mathscr{A}_g}\frac{\mathrm{d}}{\mathrm{d}X}\left(\rho_0\mathrm{Re}[u_1^*h_1] + 2h_0\dot{m}_2\right)\mathrm{d}S$$

$$+\frac{N_L^2}{\kappa}\int_{\mathscr{A}_g}\nabla_\tau\cdot\left(\rho_0\mathrm{Re}[v_1^*h_1]+2h_0\dot{\boldsymbol{m}}_{\tau_2}-\frac{\kappa\mu_0}{W_o^2}\mathrm{Re}\left[u_1^*\nabla_\tau u_1\right]\right)\mathrm{d}S$$

$$=\frac{N_L^2}{\kappa}\frac{\mathrm{d}}{\mathrm{d}X}(A_g\rho_0\mathrm{Re}[\langle u_1^*h_1\rangle]+2h_0\dot{M}_2)\,\mathrm{d}S, \tag{3.21}$$

where $\dot{M}_2 := A_g\langle\dot{m}_2\rangle$. Finally, equating the right-hand sides of (3.20) and (3.21), we obtain

$$\frac{\mathrm{d}}{\mathrm{d}X}\left(2h_0\dot{M}_2+A_g\rho_0\mathrm{Re}\left[\langle h_1u_1^*\rangle\right]-(K_0A_g+\sigma K_{s_0}A_s)\frac{S_k^2}{\kappa}\frac{\mathrm{d}T_0}{\mathrm{d}X}\right)=0. \tag{3.22}$$

The quantity within the large brackets is $\dot{H}_2$, the time-averaged total power (or energy flux) along X, and we find $\dot{H}_2$ is independent of X. Indeed, in steady state, for a cyclic refrigerator or prime mover without heat flows to the surroundings, the time-averaged energy flux along X must be independent of X. The approach used in deriving this equation is quite similar to that of Rienstra (2003).

Substituting the thermodynamic expressions (A 7) and (A 9),

$$\mathrm{d}h=T\,\mathrm{d}s+\frac{1}{\rho}\,\mathrm{d}p=C_p\mathrm{d}T+\frac{1}{\rho}(1-\beta T)\,\mathrm{d}p,$$

into (3.22), we find

$$\frac{\dot{H}_2}{A_g}=h_0\frac{\dot{M}_2}{A_g}+\tfrac{1}{2}\rho_0C_p\mathrm{Re}[\langle T_1u_1^*\rangle]+\tfrac{1}{2}(1-\beta T_0)\mathrm{Re}[p_1\langle u_1^*\rangle]$$
$$-\left(K_0+\sigma K_{s_0}\frac{A_s}{A_g}\right)\frac{S_k^2}{2\kappa}\frac{\mathrm{d}T_0}{\mathrm{d}X}. \tag{3.23}$$

Now first note that

$$\langle|F_v|^2\rangle=\mathrm{Re}\,[F_v]\,,\qquad\langle F_{kj}F_v^*\rangle=\frac{\langle F_{kj}\rangle+P_r\langle F_v^*\rangle-f_{bj}}{1+P_r},\qquad j=u,\,p, \tag{3.24}$$

where

$$f_{bj}:=\frac{1}{A_g\alpha_v^2}\int_{\Gamma_g}F_{kj}\nabla_\tau F_v^*\cdot\boldsymbol{n}_\tau\,\mathrm{d}\ell,\qquad j=u,\,p.$$

Furthermore, integrating (A 9), we find that

$$h_0=C_p(T_0-T_{ref}),$$

where T_{ref} is some reference temperature. Substituting (3.5) into (3.23) and using (3.24), we find after some manipulation

$$\frac{\dot{H}_2}{A_g}=\frac{1}{A_g}\dot{M}_2C_p\left(T_0-T_{ref}\right)+\tfrac{1}{2}\mathrm{Re}\left[p_1u_1^*\left(1-\beta T_0\frac{f_{kp}-f_v^*+f_{bp}}{(1+P_r)(1-f_v^*)}\right)\right]$$
$$+\frac{\rho_0C_p|\langle u_1\rangle|^2}{2\kappa(1-P_r)|1-f_v|^2}\frac{\mathrm{d}T_0}{\mathrm{d}X}\mathrm{Im}\left[f_v^*+\frac{f_{ku}-f_v^*+f_{bu}}{1+P_r}\right]$$
$$-\left(K_0+\sigma K_{s_0}\frac{A_s}{A_g}\right)\frac{S_k^2}{2\kappa}\frac{\mathrm{d}T_0}{\mathrm{d}X}. \tag{3.25}$$

This expression represents the total power along the X-direction (wave direction) in terms of T_0, p_1, $\langle u_1\rangle$, $\dot{M}_2$, material properties and geometry. Given $\dot{H}_2$, independent

of X, we can solve (3.25) for $\mathrm{d}T_0/\mathrm{d}X$,

$$\frac{\mathrm{d}T_0}{\mathrm{d}X} = \kappa \frac{2\dot{H}_2 - 2\dot{M}_2 C_p (T_0 - T_{ref}) - A_g \mathrm{Re}[a_1 p_1 u_1^*]}{A_g a_2 |\langle u_1 \rangle|^2 - (K_0 A_g + \sigma K_{s_0} A_s) S_k^2}, \tag{3.26}$$

where

$$a_1 := 1 - \beta T_0 \frac{f_{kp} - f_\nu^* + f_{bp}}{(1 + P_r)(1 - f_\nu^*)}, \tag{3.27}$$

$$a_2 := \frac{\rho_0 C_p}{(1 - P_r)|1 - f_\nu|^2} \mathrm{Im}\left[f_\nu^* + \frac{f_{ku} - f_\nu^* + f_{bu}}{1 + P_r} \right]. \tag{3.28}$$

It is possible to go a step further and improve the expression for the mean temperature by determining the correction term $T_{2,0}$. Integrating (3.16) and (3.17) using an appropriate Green's function, we can determine $T_{2,0}$ and $T_{s_{2,0}}$ up to some X-dependent function $T_{b_{2,0}}(= T_{b_{2,0}}(X))$. In the same way as the differential equation (3.26) for T_0 followed as a solvability condition for $T_{2,0}$ and $T_{s_{2,0}}$, we can derive an ordinary differential equation for $T_{b_{2,0}}$ as a solvability condition for the fourth-order mean temperatures $T_{4,0}$ and $T_{s_{4,0}}$. Performing this analysis, it is possible to include transverse variations into the mean temperature profile, since $T_{2,0}$ does depend on $\boldsymbol{x}_\tau$ in contrast to T_0. This can be useful when analysing heat-transfer processes in thermoacoustic heat exchangers or for short regenerators.

3.3. *Integration of* (3.14), (3.15) *and* (3.26)

In addition to T_0 solving the differential equation given in (3.26), we have that $\langle u_1 \rangle$ and p_1 satisfy the differential equations given in (3.14) and (3.15). We have already introduced the auxiliary functions a_1 and a_2 in (3.27) and (3.28). To simplify notation even more, we also introduce

$$a_3 := -\frac{\mathrm{i}}{\rho_0 c^2} \left[1 + (\gamma - 1) f_{kp} \right],$$

$$a_4 := -\frac{\beta(f_\nu - f_{ku})}{(1 - P_r)(1 - f_\nu)},$$

$$a_5 := -\frac{\mathrm{i}\rho_0}{1 - f_\nu}.$$

Consequently, we find that we have to integrate the following system of ordinary differential equations:

$$\frac{\mathrm{d}T_0}{\mathrm{d}X} = \kappa \frac{2\dot{H}_2 - 2\dot{M}_2 C_p (T_0 - T_{ref}) - A_g \mathrm{Re}[a_1 p_1 \langle u_1 \rangle^*]}{A_g a_2 |\langle u_1 \rangle|^2 - (K_0 A_g + \sigma K_{s_0} A_s) S_k^2}, \tag{3.29a}$$

$$\frac{\mathrm{d}\langle u_1 \rangle}{\mathrm{d}X} = \kappa a_3 p_1 + \left(a_4 \frac{\mathrm{d}T_0}{\mathrm{d}X} - \frac{1}{A_g} \frac{\mathrm{d}A_g}{\mathrm{d}X} \right) \langle u_1 \rangle, \tag{3.29b}$$

$$\frac{\mathrm{d}p_1}{\mathrm{d}X} = \kappa a_5 \langle u_1 \rangle. \tag{3.29c}$$

Equations (3.29) form a system of five coupled equations, determining the five real variables: $\mathrm{Re}(p_1)$, $\mathrm{Im}(p_1)$, $\mathrm{Re}(\langle u_1 \rangle)$, $\mathrm{Im}(\langle u_1 \rangle)$ and T_0. Given the total energy flux $\dot{H}_2$, the mass flux $\dot{M}_2$, the geometry, and appropriate boundary conditions in X, these equations can be integrated numerically. For example, if the stack is positioned in a resonator with the left-hand stack end at distance x_L from the closed end, then we

can impose

$$p_1(0) = \mathscr{P}\cos(kx_L), \qquad \langle u_1\rangle(0) = \frac{\mathrm{i}\mathscr{P}}{\rho_L c_L}\sin(kx_L), \qquad T_0(0) = T_L. \tag{3.30}$$

where k is the wavenumber. In addition, we can still choose the constant $\dot{H}_2$. In a steady-state situation without heat exchange with the surroundings, $\dot{H}_2 = 0$. In this case, the thermoacoustic heat flow is balanced by a return diffusive heat flow in the stack and in the gas, so that the net heat flow is zero. Alternatively, we can also impose a temperature T_R on the right-hand stack end and look for the corresponding $\dot{H}_2$ that gives the desired temperature difference.

We see that the total energy flux through the stack, the cross-sectional variations, the small-amplitude acoustical oscillations and the resulting streaming may cause $O(1)$-variations in the mean temperature. The energy flux $\dot{H}_2$ can be changed by external input or extraction of heat at the stack ends and consequently change the mean temperature profile. The acoustic oscillations affect the mean temperature via the well-known shuttling effect (see e.g. Swift 1988). With a non-zero mass flux $\dot{M}_2$, heat will be carried to the hot or cold temperature and thus affect the mean temperature also. This can either be a loss or contribute to the heat transfer.

Note that the temperature gradient scales with κ and $1/S_k^2$. Thus, in the limits $\kappa \to 0$ (short stack limit) or $S_k \to \infty$ (small velocities; heat conduction is dominating), the temperature difference across the stack will tend to zero, unless sufficient heat is supplied or extracted ($|\dot{H}_2| \gg 1$). Furthermore, the velocity and pressure gradients also scale with κ, which justifies the assumption of constant stack pressure and velocity that is commonly applied in the short-stack approximation (see e.g. Swift 1988; Wheatley, Swift & Migliori 1986).

Finally, remember that these equations are not completely independent of the parameter M_a that we used to linearize; a dimensionless number S_k still appears in the equations. In (2.16), we showed that

$$S_k = \frac{\kappa\varepsilon}{N_L M_a},$$

so that there is still a term with M_a present in the equations. Furthermore, the effect of streaming is, included also. Hence, the theory derived here is not exactly linear as it is usually claimed to be. Therefore, we prefer to use the term *weakly nonlinear* to indicate that there is still a nonlinearity involved. In the section below, we show how the equations relate to previous papers on this topic.

3.4. *Special configurations*

The system of ordinary differential equations derived above is valid for arbitrarily shaped and slowly varying cross-sections and incorporates streaming via the constant $\dot{M}_2$. Note that μ, K, c and C_p may depend on temperature. Below, we show how these equations compare to previous work on this topic. The difference with the equations above lies mainly in the chosen geometry or boundary conditions.

For pores with rotationally symmetric cross-sections, we can show that f_{ku} and f_{kp} satisfy

$$f_{kp} = \frac{f_k}{1+\varepsilon_s}, \qquad f_{ku} = \frac{f_k + \varepsilon_s f_v}{1+\varepsilon_s}, \tag{3.31}$$

where

$$\varepsilon_s := \frac{1}{\sigma}\frac{A_g\alpha_k^2 f_k}{A_s\alpha_s^2 f_s}, \qquad f_j := 1 - \langle F_j\rangle, \quad j = v, k, s.$$

Furthermore, the expressions for f_{bu} and f_{ku} simplify into

$$f_{bu} = \frac{\varepsilon_s f_\nu^*}{1+\varepsilon_s}\left(1 - \frac{f_\nu}{f_k}\right), \qquad f_{bp} = \frac{\varepsilon_s f_\nu^*}{1+\varepsilon_s}. \tag{3.32}$$

As a result, the expressions for $a_1, \ldots, a_5$ transform into the familiar form (Swift 2002)

$$a_1 := 1 - \beta T_0 \frac{f_k - f_\nu^*}{(1+P_r)(1+\varepsilon_s)(1-f_\nu^*)}, \tag{3.33}$$

$$a_2 := \frac{\rho_0 C_p}{(1-P_r)|1-f_\nu|^2}\mathrm{Im}\left[f_\nu^* + \frac{(1+\varepsilon_s f_\nu/f_k)(f_k - f_\nu^*)}{(1+P_r)(1+\varepsilon_s)}\right], \tag{3.34}$$

$$a_3 := -\frac{\mathrm{i}}{\rho_0 c^2}\left[1 + \frac{\gamma-1}{1+\varepsilon_s} f_k\right], \tag{3.35}$$

$$a_4 := \frac{\beta(f_k - f_\nu)}{(1-P_r)(1+\varepsilon_s)(1-f_\nu)}, \tag{3.36}$$

$$a_5 := -\frac{\mathrm{i}\rho_0}{1-f_\nu}. \tag{3.37}$$

For the simple two-dimensional case of parallel-plate configuration, the auxiliary functions simplify further into the expressions

$$f_\nu = \frac{\tanh(\alpha_\nu \mathscr{R}_g)}{\alpha_\nu \mathscr{R}_g}, \qquad f_k = \frac{\tanh(\alpha_k \mathscr{R}_g)}{\alpha_k \mathscr{R}_g},$$
$$f_s = \frac{\tanh(\alpha_s \mathscr{R}_s)}{\alpha_s \mathscr{R}_s}, \qquad \varepsilon_s = \frac{\phi}{\sigma}\frac{\alpha_k \mathscr{R}_g \tanh(\alpha_k \mathscr{R}_g)}{\alpha_s \mathscr{R}_s \tanh(\alpha_s \mathscr{R}_s)}.$$

Note that $\mathscr{R}_g$ and $\mathscr{R}_s$ may be X-dependent. For constant pore cross-sections, these expressions agrees with those derived by Rott (1969).

Another simplification arises, if we neglect streaming and change the boundary conditions (2.24*b*)–(2.24*d*) by simply putting $T|_{\Gamma_g} = 0$. Then $F_{ku} = F_{kp} = F_k$ and $f_{bu} = f_{bp} = 0$, and equations (3.29) simplify into those derived by Arnott *et al.* (1991) for arbitrary (constant) pore cross-sections with

$$a_1 := 1 - \beta T_0 \frac{\langle F_\nu^* \rangle - \langle F_k \rangle}{(1+P_r)\langle F_\nu^* \rangle},$$

$$a_2 := -\frac{\rho_0 C_p}{(1-P_r^2)|\langle F_\nu \rangle|^2}\mathrm{Im}\left[\langle F_k \rangle + P_r \langle F_\nu^* \rangle\right],$$

$$a_3 := -\frac{\mathrm{i}}{\rho_0 c^2}\left[1 + (\gamma-1)(1 - \langle F_k \rangle)\right],$$

$$a_4 := \frac{\beta(\langle F_\nu \rangle - \langle F_k \rangle)}{(1-P_r)\langle F_\nu \rangle},$$

$$a_5 := -\frac{\mathrm{i}\rho_0}{\langle F_\nu \rangle}.$$

We have tested our equations for the standing-wave parallel-plate configuration as described by Atchley *et al.* (1990) (TAC#3) with the geometry as given in figure 3.

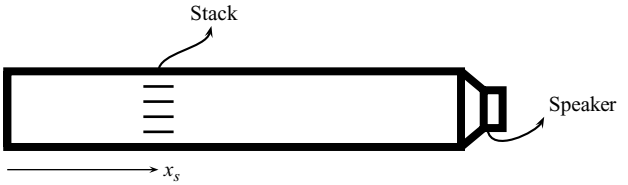

FIGURE 3. Standing-wave resonator closed on the left-hand side and with a speaker on the right-hand side. The speaker supplies acoustic power and a temperature profile arises in the stack such that $\dot{H} = 0$.

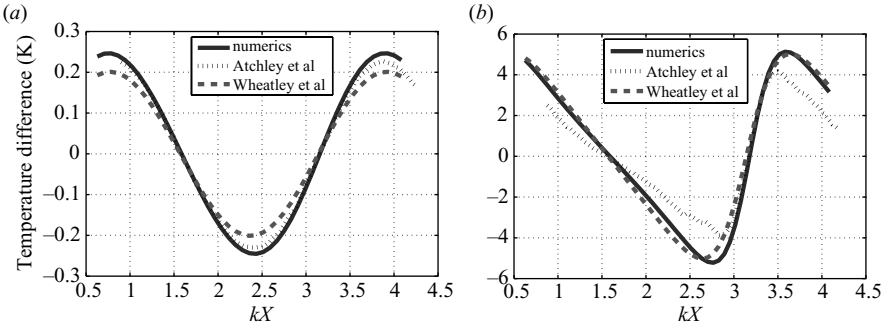

FIGURE 4. The temperature difference $T_L - T_R$ across the stack as a function of kx_s ($k = 2\pi/\lambda$), the distance of the stack centre x_s to the closed end, relative to the wavelength. —, numerical results, . . . , experimental results –·–, values predicted by Wheatley *et al.* (1986). We consider the two cases where the drive ratio D_r is (*a*) 0.28 % and (*b*) 1.99 %.

Using MATLAB's `ode45`, a Runge–Kutta type solver, we were able to integrate the equations numerically subject to the boundary conditions given in (3.30). We will compare our results to the measurements of Atchley *et al.* (1990) and the theoretical prediction of Wheatley *et al.* (1986). Wheatley *et al.* (1986) obtained an analytic expression for the temperature difference across the stack when $\dot{H} = 0$, provided the stack is short compared to the wavelength and has a plate distance that is large compared to the thermal penetration depth.

Figure 4 shows the temperature difference generated over the stack in the case $\dot{H} = 0$, and compares it to the measurements and the theoretical prediction. We consider two cases with drive ratios of 0.28 % and 1.99 %. The drive ratio is the ratio of the pressure oscillation amplitude and the mean pressure. For the low drive ratio, the fit with the measurements is remarkably good, even better than the theoretical predictions. For the high drive ratio, the fit with the theory is still quite good, but the agreement with the measurements becomes worse. Atchley *et al.* (1990) attribute this difference to uncertainties in the thermal conductivity of the stack material or possible measurement errors. It is not apparent why the theory and numerics match better for the high drive ratio. However, we do observe that if we increase the plate length or plate separation, then the agreement becomes rapidly worse.

4. Acoustic streaming

This section discusses steady second-order mass flow in the stack driven by first-order acoustic phenomena. The analysis is valid for arbitrarily shaped pores

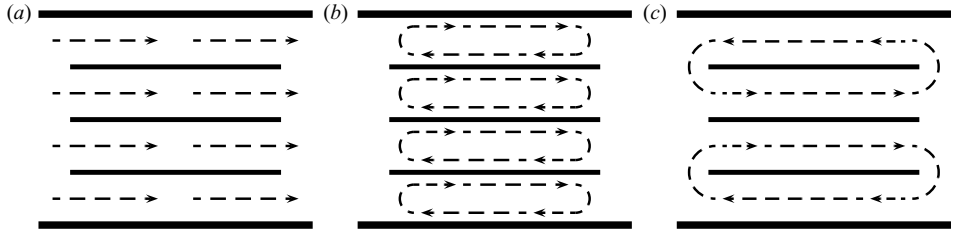

FIGURE 5. Mass streaming in stack. (*a*) Gedeon streaming. (*b*) Rayleigh streaming. (*c*) Inner streaming.

supporting a temperature gradient. Moreover, the temperature dependence of viscosity is taken into account.

There are several types of streaming that can occur simultaneously. Three kinds of streaming are shown in figure 5. *Gedeon streaming* refers to a net time-averaged mass flow through a stack pore, i.e. $\dot{M} \neq 0$, typical for looped-tube thermoacoustic devices. *Rayleigh streaming* refers to a time-averaged toroidal circulation within a stack pore driven by boundary-layer effects at the pore walls that can occur even if $\dot{M} = 0$. *Inner streaming* refers to a time-averaged toroidal circulation in the whole stack, so that the net time-averaged mass flow can differ from pore to pore both in size and direction. Inner streaming can, for example, be caused by inhomogeneities at the stack ends. Streaming effects are usually undesirable, but it was suggested by Swift (2002) that for some applications it can be useful as a substitute for heat exchangers.

We start with the continuity equation (2.17). If we time-average the equation and expand in powers of M_a, then the zeroth- and first-order terms in M_a will drop out. Consequently, we find to leading order

$$\frac{\partial}{\partial X}(\rho_0 u_{2,0}) + \rho_0 \nabla_\tau \cdot \boldsymbol{v}_{\tau_{2,0}} + \tfrac{1}{2}\mathrm{Re}\left[\frac{\partial}{\partial X}\left(\rho_1 u_1^*\right) + \nabla_\tau \cdot (\rho_1 \boldsymbol{v}_{\tau_1}^*)\right] = 0.$$

Again applying the divergence theorem and noting that $\boldsymbol{v}_\tau|_{\Gamma_g} = 0$, we can average over a cross-section to find

$$\frac{\mathrm{d}}{\mathrm{d}X}\left(A_g \rho_0 \langle u_{2,0}\rangle + \tfrac{1}{2} A_g \mathrm{Re}[\langle \rho_1 u_1^*\rangle]\right) = 0.$$

The expression between the brackets is $\dot{M}_2$, the time-averaged and cross-sectional-averaged mass flux in the X-direction. It follows that $\dot{M}_2$ is constant, which is to be expected as there is no mass transport through the stack walls. We can now express $\langle u_{2,0}\rangle$ in terms of $\dot{M}_2$ and the first-order acoustics as follows:

$$\langle u_{2,0}\rangle = \frac{1}{\rho_0}\left(\frac{\dot{M}_2}{A_g} - \tfrac{1}{2}\mathrm{Re}[\langle \rho_1 u_1^*\rangle]\right). \tag{4.1}$$

Next we turn to (2.19). Expanding in powers of M_a and ε, and averaging in time, we find to leading order in M_a and ε that

$$\nabla_\tau p_{2,0} = 0,$$

so that $p_{2,0} = p_{2,0}(X)$. Subsequently, time-averaging equation (2.18), we find to leading order

$$\nabla_\tau^2 u_{2,0} - \frac{W_o^2}{\kappa \mu_0}\frac{\mathrm{d}p_{2,0}}{\mathrm{d}X} = f, \tag{4.2}$$

where f is given by

$$f := \frac{1}{2}\frac{W_o^2}{\kappa\mu_0}\mathrm{Re}[\mathrm{i}\kappa\rho_1 u_1^* + \rho_0 \boldsymbol{v}_1^* \cdot \nabla u_1] - \tfrac{1}{2}\mathrm{Re}\left[\nabla_\tau \cdot \left(\frac{\mu_1^*}{\mu_0}\nabla_\tau u_1\right)\right].$$

The first-order acoustics collected in f can be interpreted as a source term for the streaming on the left-hand side, with the last term being characteristic for Rayleigh streaming. We can also see this as a Poisson equation for the streaming velocity $u_{2,0}$, which may be solved using a Green's function. Introducing the Green's function G_m that, for fixed $\hat{\boldsymbol{x}}_\tau \in \mathscr{A}_g(X)$, satisfies

$$\nabla_\tau G_m(\boldsymbol{x};\hat{\boldsymbol{x}}) = \delta(\boldsymbol{x}_\tau - \hat{\boldsymbol{x}}_\tau), \qquad \boldsymbol{x}_\tau \in \mathscr{A}_g(X), \tag{4.3}$$

$$G_m(\boldsymbol{x};\hat{\boldsymbol{x}}) = 0, \qquad \mathscr{S}_g(\boldsymbol{x}) = 0, \tag{4.4}$$

we have

$$u_{2,0}(\boldsymbol{x}) = \frac{W_o^2}{\kappa\mu_0}\frac{\mathrm{d}p_{2,0}}{\mathrm{d}X}\int_{\mathscr{A}_g(X)} G_m(\boldsymbol{x};\hat{\boldsymbol{x}})\,\mathrm{d}\hat{S} + \int_{\mathscr{A}_g(X)} G_m(\boldsymbol{x};\hat{\boldsymbol{x}}) f(\hat{\boldsymbol{x}})\,\mathrm{d}\hat{S}. \tag{4.5}$$

Computing the cross-sectional average, we can relate $\mathrm{d}p_{m_{20}}/\mathrm{d}X$ to $\langle u_{m,20}\rangle$ as follows:

$$\frac{\mathrm{d}p_{2,0}}{\mathrm{d}X} = \frac{\kappa\mu_0}{W_o^2}\frac{\langle u_{2,0}\rangle - \left\langle \int_{\mathscr{A}_g} G_m(\,\cdot\,;\hat{\boldsymbol{x}}) f(\hat{\boldsymbol{x}})\,\mathrm{d}\hat{S}\right\rangle}{\left\langle \int_{\mathscr{A}_g} G_m(\,\cdot\,;\hat{\boldsymbol{x}})\,\mathrm{d}\hat{S}\right\rangle}. \tag{4.6}$$

Summarizing, given the mass flux $\dot{M}_2$ and the first-order acoustics, it only remains to compute the Green's function G_m for the desired geometry. Then $\langle u_{2,0}\rangle$, $\mathrm{d}p_{2,0}/\mathrm{d}X$ and $u_{2,0}$ can be determined consecutively from (4.1), (4.6) and (4.5).

5. Acoustic power

The time-averaged acoustic power $\mathrm{d}\dot{W}_2$ used or produced in a segment of length $\mathrm{d}X$, second order in M_a, can be found from

$$\frac{\mathrm{d}\dot{W}_2}{\mathrm{d}X} = \frac{\mathrm{d}}{\mathrm{d}X}\left[A_g\overline{\langle \mathrm{Re}[p_1\mathrm{e}^{\mathrm{i}t}]\mathrm{Re}[\langle u_1\rangle\mathrm{e}^{\mathrm{i}t}]\rangle}\right]. \tag{5.1}$$

Using (2.26), we find to leading order

$$\frac{\mathrm{d}\dot{W}_2}{\mathrm{d}X} = \frac{1}{2}\frac{\mathrm{d}A_g}{\mathrm{d}X}\mathrm{Re}\left[p_1\langle u_1{}^*\rangle\right] + \frac{A_g}{2}\mathrm{Re}\left[p_1\frac{\mathrm{d}\langle u_1{}^*\rangle}{\mathrm{d}X} + \langle u_1{}^*\rangle\frac{\mathrm{d}p_1}{\mathrm{d}X}\right]. \tag{5.2}$$

Substituting (3.15) and (3.14) into (5.2) we find

$$\frac{\mathrm{d}\dot{W}_2}{\mathrm{d}X} = \frac{A_g}{2}\frac{\beta}{1-P_r}\frac{\mathrm{d}T_0}{\mathrm{d}X}\mathrm{Re}\left[\frac{f_{ku}^* - f_v^*}{(1-f_v^*)}p_1\langle u_1^*\rangle\right] - \frac{A_g}{2}\frac{\kappa(\gamma-1)}{\rho_0 c^2}\mathrm{Im}[-f_{kp}]|p_1|^2 - \frac{A_g}{2}\frac{\kappa\rho_0\mathrm{Im}\,[-f_v]}{|1-f_v|^2}|\langle u_1\rangle|^2. \tag{5.3}$$

The first term contains the temperature gradient $\mathrm{d}T_0/\mathrm{d}X$ and is called the sink or source term. It will either absorb (refrigerator) or produce (prime mover) acoustic power depending on the magnitude of the temperature gradient along the stack. This term is the unique contribution to thermoacoustics. The last two terms are the viscous

and thermal relaxation dissipation terms, respectively. These two terms arise owing to the interaction with the wall, and have a dissipative effect in thermoacoustics.

5.1. *The effect of pore size*

To see the effect of reducing the pore size, we test how (5.3) behaves for small N_L or W_o. Plugging (3.31) and (3.32) into (5.3), we find for the particular case of a parallel-plate geometry with $\varepsilon_s = 0$, that

$$\frac{\mathrm{d}\dot{W}_2}{\mathrm{d}X} = \frac{A_g}{2}\frac{\beta}{1-P_r}\frac{\mathrm{d}T_0}{\mathrm{d}X}\mathrm{Re}\left[\frac{f_k^* - f_v^*}{(1-f_v^*)}p_1\langle u_1^*\rangle\right] - \frac{A_g}{2}\frac{\kappa(\gamma-1)}{\rho_0 c^2}\mathrm{Im}\left[-f_k\right]|p_1|^2 - \frac{A_g}{2}\frac{\kappa\rho_0\mathrm{Im}\left[-f_v\right]}{|1-f_v|^2}|\langle u_1\rangle|^2. \quad (5.4)$$

For small W_o and N_L, we can show that $(f_k - f_v)/(1-f_v) = O(1)$, $\mathrm{Im}(f_k) = O(N_L^2)$, $\mathrm{Im}(f_v) = O(W_o^2)$ and $|1-f_v|^2 = O(W_o^4)$. Therefore, assuming $\mathrm{d}T_0/\mathrm{d}X$, p_1 and u_1 are $O(1)$ for small N_L and W_o, it follows that the acoustic power behaves as

$$\frac{\mathrm{d}\dot{W}_2}{\mathrm{d}X} = \frac{\mathrm{d}\dot{W}_2^s}{\mathrm{d}X} - \frac{\mathrm{d}\dot{W}_2^k}{\mathrm{d}X} - \frac{\mathrm{d}\dot{W}_2^v}{\mathrm{d}X} = O(1) - O\left(N_L^2\right) - O\left(\frac{1}{W_o^2}\right), \quad W_o, N_L \ll 1, \quad (5.5)$$

where $\dot{W}_2^s$, $\dot{W}_2^k$ and $\dot{W}_2^v$ denote the source/sink term, thermal relaxation dissipation and viscous dissipation, respectively.

Unsurprisingly, (5.5) shows that the dissipation in a regenerator ($N_L, W_o \ll 1$) is dominated by viscous dissipation and in a stack (N_L, $W_o = O(1)$) by thermal relaxation dissipation. In a regenerator, there is perfect thermal contact, but very small pores and therefore viscous dissipation will be dominant. In a stack, on the other hand, there is imperfect thermal contact, but wider pores. Thus, thermal relaxation dissipation is dominant here. Dissipation is usually undesirable, so N_L should be chosen carefully.

As an example, we go back to the standing-wave configuration as modelled by Atchley *et al.* (1990). We again consider the situation in which $\dot{H} = 0$, and position the stack near the closed end of the resonator. For a drive ratio of 2 %, we then investigate the behaviour of the acoustic power as a function of N_L. In figure 6, we have plotted the acoustic power $\Delta\dot{W}_2$ absorbed by the stack together with its source term and dissipation components. The pore radius R_g is varied and the remaining parameters are kept the same as in Atchley *et al.* (1990).

Looking at the graph of the thermal relaxation dissipation $\Delta\dot{W}_2^k$, we observe that $\Delta\dot{W}_2^k$ tends to zero for decreasing N_L, but only until $N_L \sim 0.1$. Below this value, $\Delta\dot{W}_2^k$ starts to grow rapidly again because $\Delta\dot{W}_2^k$ scales with $|p_1|^2$. As the pore size becomes smaller and smaller, the pressure drop (and also the velocity) in the stack will become larger and larger, cancelling the effect of the prefactor $\mathrm{Im}(f_k)$. For the viscous dissipation $\Delta\dot{W}_2^v$, the situation is simpler. Both $|u_1|^2$ and its prefactor will explode for small N_L, and therefore $\Delta\dot{W}_2^v$ too, as the graph clearly shows. The graph also shows that the source term is maximal for N_L close to 1. Below this value, the viscous dissipation increases dramatically and therefore, for the case considered here, N_L should not be taken smaller than 1. This is why commonly in standing-wave devices, N_L is taken close to 1.

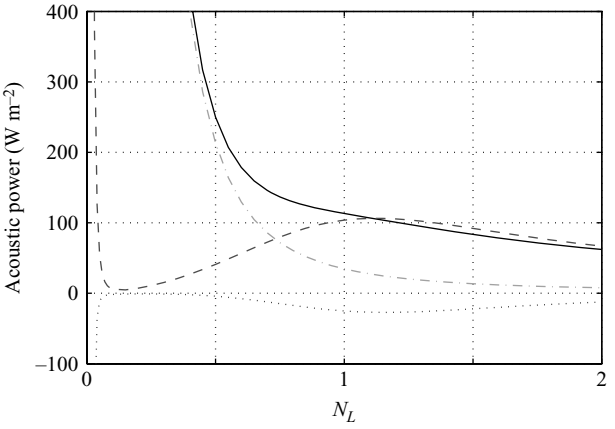

FIGURE 6. The acoustic power absorbed by the stack as a function of the Lautrec number for $\dot{H} = 0$ and a drive ratio of 2 %. The stack is positioned at 5 cm from the closed end. —, acoustic power; · · ·, source term; - - -, thermal relaxation; –·–, viscous dissipation.

6. Discussion

A weakly nonlinear theory of thermoacoustics for general porous media, applicable for both stacks and regenerators, has been developed based on a dimensional analysis and using small parameter asymptotics. Crucial assumptions for the linearization were $M_a \ll 1$ (small amplitudes) and $\mathrm{e} \ll 1$ (slow longitudinal variation). The theory is weakly nonlinear in the sense that we include second-order terms in M_a and ε (streaming and conduction). Moreover, the linearization parameters M_a and ε do not disappear completely from the system of equations (3.29), but come back in the dimensionless parameter S_k. The asymptotic theory can easily be extended to include higher-order terms, so that the higher harmonics can be included as well. Although this is a logical next step, we have not incorporated them into the analysis, as they can be treated separately and would only cloud general understanding.

In addition to M_a and ε, we have identified several other dimensionless parameters (S_k, κ, N_L) that are crucial in thermoacoustics. For these parameters, we have indicated various parameter regimes, each signifying specific geometrical or physical constraints. Furthermore, we have demonstrated the implications of varying the dimensionless parameters on the mean temperature gradient and the acoustic power produced or absorbed by the stack.

Compared to previous work on general porous media (Arnott *et al.* 1991), we have extended the model to include acoustic streaming and variations in the pore wall temperature, while allowing slowly varying cross-sections. Temperature dependence of thermal conductivity, viscosity, speed of sound and specific heat is taken into account as well. So far, the derivation of streaming has been restricted to specific geometries, whereas we consider arbitrary pore cross-sections. Furthermore, previous work on variable cross-sections has been restricted to wide tubes. Our results, on the other hand, are also valid for narrow tubes supporting a temperature gradient.

The assumption of slow variation allows us to determine the transverse variation separately from the longitudinal variation. The longitudinal variation is determined by the coupled system of five (real) ordinary differential equations given in (3.29). By systematic construction of the asymptotic theory we have found that the mean temperature T_0 follows as a solvability condition for the higher-order mean

temperature $T_{2,0}$, which has not been noted before. This procedure could be repeated to compute the higher-order temperature profile $T_{2,0}$ to provide a more accurate solution. The transverse variation of the acoustic variables is reduced to calculating Green's functions of the modified Helmholtz equation for the gas and solid and solving two additional integral equations. Lastly, the problem of determining streaming has been reduced to computing a single Green's function for the Poisson equation on the desired geometry.

This work is part of a project entitled 'High-amplitude oscillatory gas flow in interaction with solid boundaries' and is financially supported by the Technology Foundation (STW, project no. ETF.6668). We would like to thank Paul Aben, Mico Hirschberg, Fons de Waele and particularly our project leader Jos Zeegers for the valuable discussions and input.

Appendix A. Thermodynamic constants and relations

In dimensional form we have the following thermodynamic relations (taken from Chapman 2000).

$$c^2 = \left(\frac{\partial p}{\partial \rho}\right)_s, \tag{A 1}$$

$$C_p = T\left(\frac{\partial s}{\partial T}\right)_p = \left(\frac{\partial h}{\partial T}\right)_p, \tag{A 2}$$

$$C_v = T\left(\frac{\partial s}{\partial T}\right)_\rho = \left(\frac{\partial \epsilon}{\partial T}\right)_\rho, \tag{A 3}$$

$$\beta = -\frac{1}{\rho}\left(\frac{\partial \rho}{\partial T}\right)_p, \tag{A 4}$$

$$c^2\beta^2 T = C_p(\gamma - 1), \tag{A 5}$$

$$p = \rho h - \rho\epsilon, \tag{A 6}$$

$$\mathrm{d}s = \frac{C_p}{T}\,\mathrm{d}T - \frac{\beta}{\rho}\,\mathrm{d}p \quad \Rightarrow \quad s_1 = \frac{C_p}{T_0}T_1 - \frac{\beta}{\rho_0}p_1, \tag{A 7}$$

$$\mathrm{d}\rho = \frac{\gamma}{c^2}\,\mathrm{d}p - \rho\beta\,\mathrm{d}T \quad \Rightarrow \quad \rho_1 = \frac{\gamma}{c^2}p_1 - \rho_0\beta T_1, \tag{A 8}$$

$$\mathrm{d}h = T\mathrm{d}s + \frac{1}{\rho}\,\mathrm{d}p \quad \Rightarrow \quad h_1 = T_0 s_1 + \frac{p_1}{\rho_0}, \tag{A 9}$$

$$\mathrm{d}\epsilon = T\mathrm{d}s + \frac{p}{\rho^2}\,\mathrm{d}\rho \quad \Rightarrow \quad \epsilon_1 = T_0 s_1 - \frac{p_0}{\rho_0^2}\rho_1. \tag{A 10}$$

Appendix B. Green's functions

In this section, we will first show how the F-functions given in § 3.1 can be computed using Green's functions (Duffy 2001). Then we will show how the Green's functions can be computed for specific geometries.

B.1. *F-functions*

First, we introduce the Green's functions G_v and G_k. For every X we fix $\hat{\boldsymbol{x}}_\tau \in \mathscr{A}_g(X)$, set $\hat{\boldsymbol{x}} := X\boldsymbol{e}_x + \hat{\boldsymbol{x}}_\tau$, and solve for $j = v, k$

$$\mathscr{L}_j[G_j(\boldsymbol{x};\hat{\boldsymbol{x}})] = -\delta(\boldsymbol{x}_\tau - \hat{\boldsymbol{x}}_\tau), \qquad \boldsymbol{x}_\tau \in \mathscr{A}_g(X), \tag{B 1a}$$

$$G_j(\boldsymbol{x};\hat{\boldsymbol{x}}) = 0, \qquad \mathscr{S}_g(\boldsymbol{x}) = 0. \tag{B 1b}$$

Using the Green's identities, the F_j-function can be expressed in G_j $(j = v, k)$ as follows:

$$F_j(\boldsymbol{x}) = \int_{\mathscr{A}_g} G_j(\boldsymbol{x};\hat{\boldsymbol{x}})\ \mathrm{d}\hat{S}.$$

Next, we also introduce the Green's functions G_s. For fixed $\hat{\boldsymbol{x}}_\tau \in \mathscr{A}_s(X)$ we solve

$$\mathscr{L}_s\,[G_s(\boldsymbol{x};\hat{\boldsymbol{x}})] = -\delta(\boldsymbol{x}_\tau - \hat{\boldsymbol{x}}_\tau), \qquad \boldsymbol{x}_\tau \in \mathscr{A}_s(X), \tag{B 2a}$$

$$G_s(\boldsymbol{x};\hat{\boldsymbol{x}}) = 0, \qquad \mathscr{S}_g(\boldsymbol{x}) = 0, \tag{B 2b}$$

$$\nabla_\tau G_s(\boldsymbol{x};\hat{\boldsymbol{x}}) \cdot \boldsymbol{n}'_\tau = 0, \qquad \mathscr{S}_t(\boldsymbol{x}) = 0. \tag{B 2c}$$

Given g_j, it can be shown that

$$F_{kj}(\boldsymbol{x}) = \int_{\mathscr{A}_g} G_k(\boldsymbol{x};\hat{\boldsymbol{x}})\ \mathrm{d}\hat{S} - \int_{\Gamma_g} g_j(\hat{\boldsymbol{x}})\hat{\nabla}_\tau G_k(\boldsymbol{x};\hat{\boldsymbol{x}}) \cdot \boldsymbol{n}_\tau\ \mathrm{d}\hat{\ell},$$

$$F_{sj}(\boldsymbol{x}) = \int_{\Gamma_g} g_j(\hat{\boldsymbol{x}})\hat{\nabla}_\tau G_s(\boldsymbol{x};\hat{\boldsymbol{x}}) \cdot \boldsymbol{n}_\tau\ \mathrm{d}\hat{\ell}.$$

The hats in the gradients and integrals are used to indicate that the differentiation or integration is with respect to $\hat{\boldsymbol{x}}$. It only remains to determine the unknown boundary functions g_u and g_p for which we will use the boundary condition (2.24c). If we impose

$$\nabla_\tau F_{kp} \cdot \boldsymbol{n}_\tau = -\sigma \nabla_\tau F_{sp} \cdot \boldsymbol{n}_\tau, \qquad \mathscr{S}_g = 0,$$

$$\nabla_\tau (F_{kp} - P_r F_v) \cdot \boldsymbol{n}_\tau = -\sigma \nabla_\tau F_{su} \cdot \boldsymbol{n}_\tau, \qquad \mathscr{S}_g = 0,$$

then (2.24c) is satisfied to leading order. We now find that g_u and g_p are found from the following integral equations:

$$\int_{\Gamma_g} K(\boldsymbol{x};\hat{\boldsymbol{x}}) g_j(\hat{\boldsymbol{x}})\ \mathrm{d}\hat{\ell} = \Psi_j(\boldsymbol{x}), \qquad \mathscr{S}_g(\boldsymbol{x}) = 0, \qquad j = u, p, \tag{B 3}$$

where Ψ_u, Ψ_p and K are defined as

$$\Psi_p(\boldsymbol{x}) = \int_{\mathscr{A}_g} \nabla_\tau G_k(\boldsymbol{x};\hat{\boldsymbol{x}}) \cdot \boldsymbol{n}_\tau\ \mathrm{d}\hat{S},$$

$$\Psi_u(\boldsymbol{x}) = \int_{\mathscr{A}_g} \nabla_\tau\,(G_k(\boldsymbol{x};\hat{\boldsymbol{x}}) - P_r G_v(\boldsymbol{x};\hat{\boldsymbol{x}})) \cdot \boldsymbol{n}_\tau\ \mathrm{d}\hat{S},$$

$$K(\boldsymbol{x};\hat{\boldsymbol{x}}) = \nabla_\tau(\hat{\nabla}_\tau(G_k(\boldsymbol{x};\hat{\boldsymbol{x}}) - \sigma\phi G_s(\boldsymbol{x};\hat{\boldsymbol{x}})) \cdot \boldsymbol{n}_\tau) \cdot \boldsymbol{n}_\tau.$$

In most cases, these integral equations are not trivially solved. Arnott *et al.* (1991) avoided this problem by setting the wall temperature equal to zero, i.e. $g_u = g_p = 0$, which is a reasonable assumption for most practical cases. In that case, $F_{su} = F_{sp} = 1$

n	Laplace: ∇_τ^2	Modified Helmholtz: $\nabla_\tau^2 - 1/\alpha_j^2$
1	$-\frac{1}{2}\lvert\boldsymbol{x}_\tau - \hat{\boldsymbol{x}}_\tau\rvert$	$\frac{1}{2\alpha_j}\exp(-\alpha_j\lvert\boldsymbol{x}_\tau - \hat{\boldsymbol{x}}_\tau\rvert)$
2	$-\frac{1}{2\pi}\log\lvert\boldsymbol{x}_\tau - \hat{\boldsymbol{x}}_\tau\rvert$	$\frac{1}{2\pi}K_0(-\alpha_j\lvert\boldsymbol{x}_\tau - \hat{\boldsymbol{x}}_\tau\rvert)$

TABLE 3. Free-space Green's functions on $\mathbb{R}^n$.

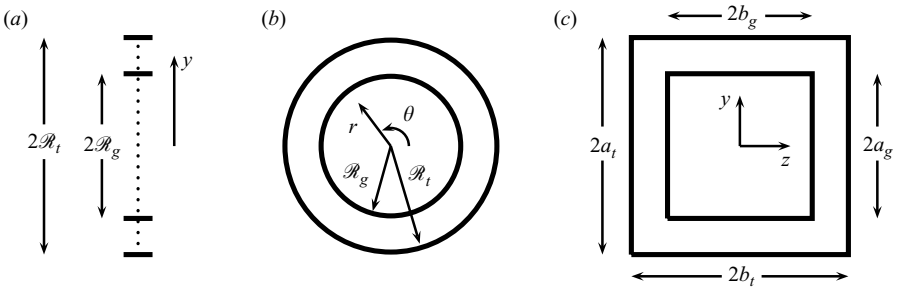

FIGURE 7. Various stack geometries. (*a*) Parallel plates. (*b*) Circular cross-sections. (*c*) Rectangular cross-sections.

and $F_{kp} = F_{ku} = F_k$ as introduced by Arnott *et al.* (1991). The second case for which the solution is simple is when $\mathscr{A}_g$ is rotationally symmetric, i.e. the case discussed in § 3.4. Then K and the g_i-functions will be constant on $\Gamma_g(X)$ and we find

$$g_i = \frac{\Psi_i}{K}, \qquad i = u, p. \tag{B 4}$$

For the general case, we must resort to the general theory of integral equations. For example, a solution can be attempted in the form of a sum of orthogonal basis functions.

B.2. *Green's functions for various stack geometries*

There is more than one way to determine the Green's functions G_j. One way is using *the method of images* (Duffy 2001). The method of images adds homogeneous solutions to the free-space Green's function in such a way that their sum satisfies the right boundary conditions. The free-space Green's functions are given in table 3 and are fundamental solutions of the Laplace and modified Helmholtz equations that have suitable behavior at infinity.

As an example, we consider the case $n = 1$ where we have a geometry as shown in figure 7(*a*), so that $\boldsymbol{x}_\tau = y$. Define

$$\Phi_j(\boldsymbol{x}, \hat{\boldsymbol{x}}) := \frac{1}{2\alpha_j}\exp(-\alpha_j|y - \hat{y}|), \quad j = \nu, k, s.$$

We now want to add a homogeneous function such that the resulting function vanishes at Γ_g. Introducing sources at the reflection points $2\mathscr{R}_g - \hat{y}$ and $-2\mathscr{R}_g - \hat{y}$, we can cancel the contribution of $\hat{y}$ on Γ_g. However, to eliminate the contributions of $2\mathscr{R}_g - \hat{y}$ and $-2\mathscr{R}_g - \hat{y}$ we have to introduce even more sources. Continuing in this way, we can write the Green's functions G_j $(j = \nu, k)$ in the form of an infinite

sum,

$$G_j(\boldsymbol{x}, \hat{\boldsymbol{x}}) = \sum_{k=-\infty}^{\infty} (\Phi_j[\boldsymbol{x}; \boldsymbol{a}_k] - \Phi_j[\boldsymbol{x}; \boldsymbol{b}_k]), \qquad j = m, \nu, k, \tag{B 5}$$

where

$$\boldsymbol{a}_k = (X, \hat{y} + 4k\mathscr{R}_g), \qquad \boldsymbol{b}_k = (X, -\hat{y} + (4k-2)\mathscr{R}_g).$$

Similarly, we can show that in the solid, G_s is given by the sum

$$G_s(\boldsymbol{x}, \hat{\boldsymbol{x}}) = \sum_{k=-\infty}^{\infty} (-1)^k (\Phi_s[\boldsymbol{x}; \boldsymbol{a}_{sk}] - \Phi_s[\boldsymbol{x}; \boldsymbol{b}_{sk}]), \tag{B 6}$$

where

$$\boldsymbol{a}_{sk} = (X, \hat{y} + 2k(\mathscr{R}_t - \mathscr{R}_g)), \qquad \boldsymbol{b}_{sk} = (X, -\hat{y} + 2k(\mathscr{R}_t - \mathscr{R}_g) + 2\mathscr{R}_g).$$

For $n = 2$, we could again use a similar strategy as for the case $n = 1$. Instead we will employ a different approach that is also used by Duffy (2001) and that solves for the Green's functions by expanding in eigenfunctions. For circular pores, this leads to the following expressions:

$$G_m(\boldsymbol{x}; \hat{\boldsymbol{x}}) = \frac{1}{\pi \mathscr{R}_g^2} \sum_{n=-\infty}^{\infty} \sum_{i=1}^{\infty} \frac{J_n(k_{ni}\hat{r}) J_n(k_{ni} r)}{k_{ni}^2 J_n'^2(k_{ni}\mathscr{R}_g)} \cos[n(\theta - \hat{\theta})], \tag{B 7}$$

$$G_j(\boldsymbol{x}; \hat{\boldsymbol{x}}) = \frac{1}{\pi \mathscr{R}_g^2} \sum_{n=-\infty}^{\infty} \sum_{i=1}^{\infty} \frac{\alpha_j^2 J_n(k_{ni}\hat{r}) J_n(k_{ni} r)}{\left(k_{ni}^2 - \alpha_j^2\right) J_n'^2\left(k_{ni}\mathscr{R}_g\right)} \cos[n(\theta - \hat{\theta})], \qquad j = k, \nu, \tag{B 8}$$

$$G_s(\boldsymbol{x}; \hat{\boldsymbol{x}}) = \frac{2}{\pi} \sum_{n=-\infty}^{\infty} \sum_{i=1}^{\infty} \frac{\alpha_j^2 \mathscr{J}_{ni}(l_{ni}\hat{r}) \mathscr{J}_{ni}(l_{ni} r) \cos[n(\theta - \hat{\theta})]}{\epsilon_n \left(k_{ni}^2 - \alpha_j^2\right) \left[\mathscr{R}_t^2 \mathscr{J}_{ni}'^2(l_{ni}\mathscr{R}_t) - \mathscr{R}_g^2 \mathscr{J}_{ni}'^2(l_{ni}\mathscr{R}_g)\right]}, \tag{B 9}$$

where the prime denotes differentiation and

$$\mathscr{J}_{ni}(r) = Y_n(l_{ni}\mathscr{R}_g) J_n(r) - J_n(l_{ni}\mathscr{R}_g) Y_n(r), \qquad \epsilon_n = \begin{cases} 2, & n = 0, \\ 1, & n > 0, \end{cases}$$

and J_n and Y_n are the Bessel functions of the first and second kind, respectively. Furthermore, the eigenvalues k_{ni} and l_{ni} are computed from

$$J_n(k_{ni}\mathscr{R}_g) = 0, \qquad \frac{\mathrm{d}\mathscr{J}_n}{\mathrm{d}r}(l_{ni}\mathscr{R}_t) = 0.$$

For rectangular pores, we obtain the following Green's functions:

$$G_m = \frac{4}{a_g b_g} \sum_{i,n=1}^{\infty} \frac{g_{in}}{i^2\pi^2/a_g^2 + n^2\pi^2/b_g^2}, \tag{B 10}$$

$$G_j = \frac{4}{a_g b_g} \sum_{i,n=1}^{\infty} \frac{\alpha_j^2 g_{in}}{i^2\pi^2/a_g^2 + n^2\pi^2/b_g^2 - 4\alpha_j^2}, \qquad j = k, \nu, \tag{B 11}$$

$$G_s = \frac{4}{(a_s)(b_s)} \sum_{i,n\,\mathrm{odd}}^{\infty} \frac{\alpha_s^2 s_{in}}{i^2\pi^2/(a_s)^2 + n^2\pi^2/(b_s)^2 - 4\alpha_s^2}. \tag{B 12}$$

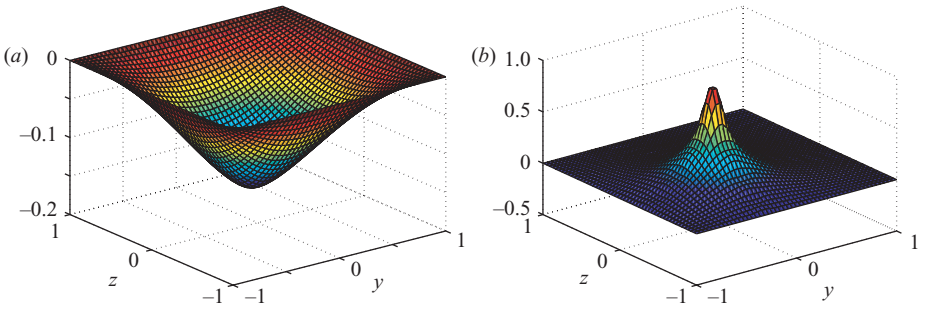

FIGURE 8. The Green's function G_j for the Helmholtz equation over a rectangular region with Dirichlet boundary conditions on the sides when $a_g = b_g = 1$, $\alpha_j = 1 + \mathrm{i}$, and $\hat{y} = \hat{z} = -0.3$. (*a*) $\mathrm{Re}(G_j)$ (*b*) $\mathrm{Im}(G_j)$.

with eigenfunctions

$$g_{in}(\boldsymbol{x};\hat{\boldsymbol{x}}) = \sin\left[i\pi\frac{y+a_g}{2a_g}\right]\sin\left[i\pi\frac{\hat{y}+a_g}{2a_g}\right]\sin\left[n\pi\frac{z+b_g}{2b_g}\right]\sin\left[n\pi\frac{\hat{z}+b_g}{2b_g}\right],$$

$$s_{in}(\boldsymbol{x};\hat{\boldsymbol{x}}) = \sin\left[\frac{i\pi}{2}\frac{y-a_g}{a_s}\right]\sin\left[\frac{i\pi}{2}\frac{\hat{y}-a_g}{a_s}\right]\sin\left[\frac{n\pi}{2}\frac{z-b_g}{b_s}\right]\sin\left[\frac{n\pi}{2}\frac{\hat{z}-b_g}{b_s}\right],$$

where $a_s = a_t - a_g$ and $b_s = b_t - b_g$. As an example of what such a Green's function may look like, we have plotted G_j in figuer 8 as a function of y and z on the unit square.

REFERENCES

ARNOTT, W. P., BASS, H. E. & RASPET, R. 1991 General formulation of thermoacoustics for stacks having arbitrarily shaped pore cross sections. *J. Acoust. Soc. Am.* **90**, 3228–3237.

ATCHLEY, A. A., HOFLER, T., MUZZERALL, M. L., KITE, M. D. & AO, C. 1990 Acoustically generated temperature gradients in short plates. *J. Acoust. Soc. Am.* **88**, 251.

AURIAULT, J. L. 1983 Heterogeneous medium. Is an equivalent macroscopic description possible? *Intl J. Engng Sci.* **29**, 785–795.

AURIAULT, J. L. 2002 Upscaling heterogeneous media by asymptotic expansions. *J. Engng Mech.* **128**, 817–822.

BACKHAUSS, S. & SWIFT, G. W. 2000 A thermoacoustic Stirling heat engine: detailed study. *J. Acoust. Soc. Am.* **107**, 3148–3166.

BAILLIET, H., GUSEV, V., RASPET, R. & HILLER, R. A. 2001 Acoustic streaming in closed thermoacoustic devices. *J. Acoust. Soc. Am.* **110**, 1808–1821.

BUCKINGHAM, E. 1914 On physically similar systems: illustrations of the use of dimensional equations. *Phys. Rev.* pp. 345–376.

CHAPMAN, C. J. 2000 *High Speed Flow*. Cambridge University Press.

CHAPMAN, S. & COWLING, T. G. 1939 *The Mathematical Theory of Non-uniform Gases; an Account of the Kinetic Theory of Viscosity, Thermal Conduction, and Diffusion in Gases*. Cambridge University Press.

DUFFY, D. G. 2001 *Green's Functions with Applications*. Chapman & Hall.

GARRETT, S. L. 2004 Thermoacoustic engines and refrigerators. *Am. J. Phys.* **72**, 11–17.

GIFFORD, W. E. & LONGSWORTH, R. C. 1966 Surface heat pumping. *Adv. Cryog. Engng* **1**, 302.

GUSEV, V., BAILLIET, H., LOTTON, P. & BRUNEAU, M. 2000 Asymptotic theory of nonlinear acoustic waves in a thermoacoustic prime-mover. *Acustica* **86**, 25–38.

HORNUNG, U. (ED.) 1997 *Homogenization and Porous Media*. Springer.

KAMIŃSKI, M. M. 2002 On probabilistic viscous incompressible flow of some composite fluids. *Comput. Mech.* **28**, 505–517.

KIRCHHOFF, G. 1868 Ueber den Einfluss der Wärmteleitung in einem Gas auf die Schallbewegung. *Annln Phys.* **134**, 177.

KRAMERS, H. A. 1949 Vibrations of a gas column. *Physica* **15**, 971.

KRÖNER, E. 1986 *Modeling Small Deformations of Polycrystals*, chap. Statistical modeling. Elsevier.

LANDAU, L. D. & LIFSHITZ, E. M. 1959 *Fluid Mechanics*. Pergamon.

LICHT, JR., W. & STECHERT, D. G. 1944 The variation of the viscosity of gases and vapors with temperature. *J. Phys. Chem.* **48**, 23–47.

MATTHEIJ, R. M. M., RIENSTRA, S. W. & TEN THIJE BOONKKAMP, J. H. M. 2005 *Partial Differential Equations: Modeling, Analysis, Computation*. SIAM, Philadelphia.

MERKLI, P. & THOMANN, H. 1975 Thermoacoustic effects in a resonant tube. *J. Fluid Mech.* **70**, 161.

NYBORG, W. L. M. 1965 *Physical Acoustics*, vol. IIB, chap. Acoustic streaming, p. 265. Academic.

OLSON, J. R. & SWIFT, G. W. 1994 Similitude in thermoacoustics. *J. Acoust. Soc. Am.* **95**, 1405–1412.

OLSON, J. R. & SWIFT, G. W. 1997 Acoustic streaming in pulse-tube refrigerators: tapered pulse tubes. *Cryogenics* pp. 769–776.

POESSE, M. E. & GARRETT, S. L. 2000 Performance measurements on a thermoacoustic refrigerator driven at high amplitudes. *J. Acoust. Soc. Am.* **107**, 2480–2486.

QUINTARD, M. & WHITAKER, S. 1993 Transport in ordered and disordered porous media: volume-averaged equations, closure problems, and comparison with experiments. *Chem. Engng Sci.* **48**, 2537–2564.

RAYLEIGH, LORD 1945 *Theory of Sound*, Vol. 2 II, Dover.

RIENSTRA, S. 2003 Sound propagation in slowly varying lined flow ducts of arbitrary cross-section. *J. Fluid Mech.* **495**, 157–173.

RIJKE, P. L. 1859 Notiz über eine neue Art, die in einer an beiden Enden offenen Rohre enthaltene Lift in Schwingungen zu versetzen. *Annln Phys.* **107**, 339.

ROH, H., RASPET, R. & BASS, H. E. 2007 Parallel capillary-tube-based extension of thermo-acoustic theory for random porous media. *J. Acoust. Soc. Am.* **121**, 1413–1422.

ROTT, N. 1969 Damped and thermally driven acoustic oscillations in wide and narrow tubes. *z. Angew. Math. Phy.* **20**, 230–243.

ROTT, N. 1973 Thermally driven acoustic oscillations. Part II: Stability limit for helium. *z. Angew. Math. Phy.* **24**, 54–72.

ROTT, N. 1974 The influence of heat conduction on acoustic streaming. *z. Angew. Math. Phy.* **25**, 417–421.

ROTT, N. 1975 Thermally driven acoustic oscillations. Part III: Second-order heat flux. *z. Angew. Math. Phy.* **26**, 43–49.

ROTT, N. 1980 Thermoacoustics. *Adv. Appl. Mech.* **20**, 135–175.

ROTT, N. & ZOUZOULAS, G. 1976 Thermally driven acoustic oscillations. Part IV: Tubes with variable cross-section. *z. Angew. Math. Phy.* **27**, 197–224.

SONDHAUSS, C. 1850 Ueber die Schallschwingungen der Luft in erhitzten Glasröhren und in gedeckten Pfeifen von ungleicher Weite. *Annln Phys.* **79**, 1.

SWIFT, G. W. 1988 Thermoacoustic engines. *J. Acoust. Soc. of Am.* **84**, 1146–1180.

SWIFT, G. W. 1992 Analysis and performance of a large thermoacoustic engine. *J. Acoust. Soc. Am.* **92**, 1551–1563.

SWIFT, G. W. 2002 *A Unifying Perspective for Some Engines and Refrigerators*. Acoustical Society of America.

TACONIS, K. W. 1949 Vapor–liquid equilibrium of solutions of ^{3}He in ^{4}He. *Physica* **15**, 738.

VAN DYKE, M. 1987 Slow variations in continuum mechanics. *Adv. Appl. Mech.* **25**, 1–45.

WAXLER, R. 2001 Stationary velocity and pressure gradients in a thermoacoustic stack. *J. Acoust. Soc. Am.* **109**, 2739.

WHEATLEY, J. C., SWIFT, G. W. & MIGLIORI, A. 1986 The natural heat engine. *Los Alamos Science* pp. 2–33.

ZAOUI, A. 1987 *Homogenization Techniques for Composite Media*, chap. Approximate statistical modelling and applications. Berlin.